Title:

Gut microbiomes of Malawian twin pairs discordant for kwashiorkor

Authors:

Michelle I. Smith[1†], Tanya Yatsunenko[1†], Mark J. Manary[2,3], Indi Trehan[2], Rehab Mkakosya[4], Jiye Cheng[1], Stephen S. Rich[5], Patrick Concannon[5], Josyf C. Mychaleckyj[5], Jie Liu[6], Eric Houpt[6], Jia V. Li[7], Elaine Holmes[7], Jeremy Nicholson[7] , Dan Knights[8,9], Luke K. Ursell[10], Rob Knight[8,9,10,11], and Jeffrey I. Gordon[1,*]

Affiliations:

[1]Center for Genome Sciences and Systems Biology, Washington University in St. Louis, St. Louis, MO 63108, USA.
[2]Department of Pediatrics, Washington University in St. Louis, St. Louis, MO 63108, USA and the Departments of Community Health, and Pediatrics and Child Health, University of Malawi College of Medicine, Blantyre, Malawi.
[3]USDA Children's Nutrition Research Center, Baylor College of Medicine, Houston, Texas 77030, USA.
[4]Department of Microbiology, College of Medicine, University of Malawi, P/B 360, Chichiri, Blantyre 3, Malawi.
[5]Center for Public Health Genomics, University of Virginia, Charlottesville, VA 22904, USA.
[6]Division of Infectious Diseases and International Health, University of Virginia, Charlottesville, VA 22908, USA,
[7]Biomolecular Medicine, Department of Surgery and Cancer, Faculty of Medicine, Imperial College London, London SW7 2AZ, UK.
[8]Department of Computer Science, Univ. of Colorado, Boulder, CO 80309, USA.
[9]Biofrontiers Institute, University of Colorado, Boulder, CO 80309, USA.
[10]Department of Chemistry and Biochemistry, University of Colorado, Boulder, CO 80309, USA.
[11]Howard Hughes Medical Institute, Univ. of Colorado, Boulder, CO 80309, USA.

[*]Correspondence to: jgordon@wustl.edu

[†]These authors contributed equally to this work.

Abstract:

Kwashiorkor, an enigmatic form of severe acute malnutrition (SAM), is the consequence of inadequate nutrient intake plus additional environmental insults. To investigate the role of the gut microbiome, we studied 317 Malawian twin pairs during the first 3 years of life; 50% of twin pairs remained well-nourished, while 43% became discordant and 7% manifested concordance for acute malnutrition. Discordance was not affected by zygosity or gender. Both co-twins discordant pairs with kwashiorkor were treated with a peanut-based, ready-to-use therapeutic food (RUTF). Time-series metagenomic studies of 9 same-gender pairs who remained well-nourished and 13 who became discordant for kwashiorkor revealed that RUTF produced a transient maturation in the representation of metabolic functions in kwashiorkor microbiomes that regressed shortly after cessation of RUTF. Previously frozen fecal communities from several discordant pairs were each transplanted into gnotobiotic mice given a representative, nutrient-deficient Malawian diet followed by RUTF and then the Malawian diet. Metagenomic, mass spectrometric and NMR studies revealed that the combination of a Malawian diet and a kwashiorkor microbiome produced marked weight loss in the gnotobiotic mice, accompanied by perturbations in amino acid, carbohydrate and intermediary metabolism that were only transiently ameliorated with RUTF. These findings implicate the gut microbiome as a causal factor in kwashiorkor and suggest that additional nutritional support may be required to correct persistent metabolic defects arising from microbiome dysfunction in malnourished children.

One Sentence Summary:

Time series studies of 317 Malawian twins pairs aged 0-3 years, including those discordant for kwashiorkor, plus analyses of the effects of transplanting gut

microbiomes from twins discordant for kwashiorkor into gnotobiotic mice fed a nutrient-deficient Malawian diet or a ready-to-use therapeutic food, reveal the importance of environmental factors, notably the gut microbial community and diet, in development of this form of severe acute malnutrition.

Main Text:

Malnutrition is the leading cause of child mortality worldwide (*1)*. Moderate acute malnutrition (MAM) refers to simple wasting with a weight-for-height Z score (WHZ) less than two but greater than three standard deviations below the median defined by World Health Organization (WHO) Child Growth Standards (*2)*. Severe acute malnutrition (SAM) refers to either marasmus, which is extreme wasting with WHZ scores less than -3, or kwashiorkor. Kwashiorkor is a virulent form of SAM characterized by generalized edema, hepatic steatosis, skin rashes and ulcerations, and anorexia (*3,4*). The cause of kwashiorkor remains obscure. Speculation regarding its pathogenesis has focused on inadequate protein intake and/or excessive oxidative stress, but substantial evidence to refute these hypotheses has come from epidemiologic surveys and clinical trials (*5-8*). We recently conducted a comparative metagenomic study of the gut microbiomes of 531 healthy infants, children and adults, representing 151 families, living in the USA, Venezuela, and Malawi; it revealed a maturational program where the proportional representation of genes encoding functions related to micro- and macronutrient biosynthesis and metabolism changes as healthy infants and children develop (*9*). Together, these observations give rise to the following testable hypotheses: (i) the gut microbiome provides essential functions needed for healthy postnatal growth and development; (ii) disturbances in microbiome assembly and function (e.g., those prompted by enteropathogen infection), affect the risk for kwashiorkor; and (iii) in a self-reinforcing pathogenic cascade, malnutrition affects gut microbiome functions involved in determining nutritional status, thus further worsening health status. A challenge is that there may be a number of gut microbiome

configurations associated with kwashiorkor among different hosts and even within a given host over time. Moreover, microbiome configurations associated with kwashiorkor may be differentially affected by therapeutic food interventions and features that are reconfigured during treatment may not persist after its withdrawal.

To begin to address some of these hypotheses, and challenges we performed a longitudinal comparative metagenomic study of the fecal microbiomes of monozygotic (MZ) and dizygotic (DZ) twin pairs born in Malawi who became discordant for SAM. Malawi has one of the highest infant mortality rates in the world (*1*), with 35% of childhood deaths associated with malnutrition (*10*). We reasoned that a healthy (well-nourished) co-twin in a twin pair discordant for kwashiorkor represented a very desirable control given his/her genetic relatedness to the affected co-twin, and their similar exposures to diet, the microbiota of family members and other microbial reservoirs in their shared early environment. A RUTF composed of peanut paste, sugar, vegetable oil and milk fortified with vitamins and minerals has become the international standard of treatment for SAM (*11*). In Malawi, the standard of care for twins discordant for kwashiorkor is to treat both co-twins with RUTF to limit food sharing; this practice allowed us to compare and contrast their microbiomes prior to, during and after treatment. Following each child in a twin pair prospectively permitted each individual to serve as his or her own control. Moreover, if there are many different routes to disrupted microbiome structure/function, then each discordant twin pair could provide a 'vignette' of underlying pathology. Finally, as an additional set of controls, we defined temporal variation of the fecal microbiomes in twin pairs who remained well-nourished, lived in the same geographic locations as discordant pairs, and never received RUTF.

A total of 317 twin pairs less than 3 years old were enrolled, regardless of their health status, from five villages (Makhwira, Mitondo, M'biza, Chamba, Mayaka) in the southern region of Malawi. The average age at enrollment was 9±6 months (mean ± SD). All but 19 twin pairs were breastfeeding at the time of enrollment (age at cessation of breastfeeding, 18±5 months). Children were followed until they were 36 months old. Zygosity testing (see *Methods*) revealed that 46 (15%) of twin pairs were monozygotic. The percentage of same-gender twin pairs in the cohort was significantly higher than opposite gender pairs [$p<10^{-8}$, Binomial test, probability of success = 0.66, Confidence Interval = (0.61, 0.71), **table S1A**]. We did not have information about the order in which each child in a twin pair was born.

Nutritional status was assessed monthly. Every attempt was made to collect a fecal sample every 8 weeks until 1 year of age, and every 12 weeks thereafter. Fecal samples were frozen in cryogenic storage containers at -190°C within 10 min after they were produced, and stored at -80°C. Kwashiorkor was diagnosed based on the presence of bilateral pitting pedal edema (*12*). Marasmus was diagnosed when an infant or child had a WHZ less than -3. Children with WHZ scores between -2 and -3 were classified as MAM (*2*). Among 244 mothers tested for HIV, 14 were positive; of the 147 children surveyed, only 1 was positive.

Twin pairs who developed kwashiorkor or marasmus immediately received RUTF; those with MAM were given a soy-peanut ready-to-use supplementary food (*13*). After diagnosis with SAM, anthropometry was assessed and a fecal sample was collected every two weeks until the child recovered (defined as WHZ score greater than -2 and no edema).

Fifty percent of twin pairs remained well-nourished throughout the study while 43% became discordant and 7% manifested concordance for acute malnutrition (**table S1A**). The prevalence of discordant compared to concordant phenotypes was significant ($p<10^{-15}$, Binomial and Chi-squared tests). MAM was significantly more frequent than SAM, affecting 81 (60%) of the 135 discordant twin pairs (p=0.02, Chi-square test). Of the 634 children in the study, 7.4% developed kwashiorkor, 2.5% marasmus, and 13.9% MAM; 10% had multiple episodes of malnutrition with the most frequent combination being marasmus and MAM (5.4% of the children, **table S1B**). The average age at presentation with marasmus was 11±4 months; the corresponding ages for kwashiorkor and MAM were 16±7 and 14±7 months, respectively. Children with marasmus suffered significantly more episodes of diarrhea than did those with kwashiorkor or MAM ($p<0.05$; **table S1C**).

The highest proportion of deaths was found in twin pairs discordant for marasmus compared to those discordant for kwashiorkor or MAM (p=0.0027, Chi-square test): a co-twin died during the study in 43% of the twin pairs who were discordant for marasmus compared to 9% in twin pairs discordant for kwashiorkor and 14% in those discordant for MAM (**table S1A**). The majority of deaths were attributed to diarrhea, malaria or pneumonia. In 120 of the 317 (37.9%) sampled families, at least one child (not a twin) had died at some point before our study; these deaths were not significantly more frequent in families of twins affected with SAM.

There was no significant relationship between concordance for acute malnutrition and zygosity (**table S1A**), nor did we find significant differences in the number of MZ versus DZ twin pairs affected with kwashiorkor, marasmus, or MAM in

our cohort (**table S1A**, Chi-squared and Fisher's exact tests). Taking all 135 discordant pairs into account, there was no statistically significant difference in the incidence of discordance for kwashiorkor, marasmus, or MAM in MZ versus DZ twin pairs (**table S1A**). In addition, we did not find any association between gender or geographic location and the type or incidence of malnutrition or in the discordance rate for MAM or SAM among twin pairs (Chi-squared and Fisher's exact tests, **table S1B,C**).

Metagenomic studies of the fecal microbiomes of same-gender twins discordant for kwashiorkor

For the current study, we chose to focus on the microbiomes of children with kwashiorkor because survival of both members of a twin pair was significantly higher than with marasmus, onset occurred at a later age allowing us to better assess the state of maturation of the microbiome, the duration of RUTF treatment was more uniform than in cases of marasmus, and there was a lower incidence of relapse to SAM. Analysis of the microbiomes of children with marasmus will be the subject of another study.

We selected 9 same gender twin pairs who remained well-nourished in our study cohort and 13 of 19 same gender twin pairs who became discordant for kwashiorkor for metagenomic analyses of their microbiomes [n=5 MZ and 4 DZ healthy pairs; 7 MZ and 6 DZ pairs discordant for kwashiorkor; for 12 of the 13 discordant pairs, there was a single episode of SAM during the study period; see **table S2A** for additional information about subjects and samples].

Comparison of fecal microbiomes across healthy twin pairs and twin pairs discordant for kwashiorkor - Total fecal DNA was used for multiplex shotgun pyrosequencing (454 FLX

Titanium chemistry; n=308 samples). Reads were annotated by comparison to the KEGG database (**table S2A**) and to a database of 462 sequenced human gut microbes (**table S3**). To compare functional gene profiles across all 308 fecal samples, we calculated Hellinger distances from KEGG enzyme commission number (EC) assignments. Principal coordinates analysis (PCoA) of Hellinger distances was used to visualize variation in this dataset (**Fig. 1A** and **fig. S1**). Principal coordinate 1 (PC1), which explained the largest amount of variation (17%), was strongly associated with age and family membership (linear mixed-effects model, **table S4**). Hellinger distances were calculated using KEGG ECs present in 93 fecal microbiome samples obtained from 9 healthy twin pairs surveyed between three weeks and 24.5 months of age. We found that on average the degree of intrapersonal variation in a co-twin was not smaller than the variation between co-twins (**fig. S2**). Similar to twins who remained healthy, the temporal variation within a co-twin member of a discordant twin pair was equal to the variation between co-twins, but still smaller than to unrelated children (**fig. S2**).

Since age encompasses a variety of metabolic and dietary changes, we used the positions of microbiomes along PC1 in the KEGG EC-based PCoA plot to assess functional 'maturation' of the microbiomes of twin pairs who remained healthy and twin pairs who became discordant for kwashiorkor. When microbiomes from three consecutive time points from twins who remained healthy were plotted along PC1, there was a steady progression towards a more mature configuration (**Fig. 1B**). A similar result was observed in healthy co-twins from discordant twin pairs: fecal microbiomes 1 month after cessation of RUTF were significantly more mature compared to before RUTF ($p<0.05$, Friedman test with Dunn's post-hoc comparison; **Fig. 1C**). This was not

the case for their siblings with kwashiorkor: their fecal microbiomes, sampled prior to, 2 and 4 weeks after initiation of, and 1 month following cessation of RUTF, did not show significant differences in their state of functional maturation (**Fig. 1C**).

We examined differences in functional gene content in the fecal microbiomes of each discordant twin pair individually using Fisher's exact test. To do so, the representation of KEGG ECs were compared between a healthy and malnourished co-twin within each family at the time of presentation with kwashiorkor, two weeks into RUTF treatment, and 1 month after termination of RUTF. We did not identify any ECs that were significantly different across *all* 13 twin pairs; each discordant twin pair had a unique collection of ECs that were significantly different at each point of comparison (see **table S5** for EC differences shared among subsets of the 13 twin pairs).

These associations between the configurations of gut microbial communities and health status do not establish whether the microbiome is a causal factor in the pathogenesis of kwashiorkor. Moreover, because of the high intra- and interpersonal variation in the composition of the gut microbiome in the first three years of life, identifying the mechanisms by which gut microbiome may contribute to kwashiorkor is daunting. We have previously used metagenomic methods to show that a fecal microbial community from a single human donor can be replicated with a high degree of fidelity in multiple germ-free mouse recipients (*14,15*): these gnotobiotic animals can be given the same diets as those consumed by the donor, and can be followed over time under highly controlled environmental conditions that are not achievable in clinical studies. We reasoned that transplanting previously frozen fecal microbial communities, obtained from twin pairs at the time one of the co-twins presented with kwashiorkor,

would allow us to assess the degree to which donor phenotypes could be transmitted via their gut microbiomes, and to identify features of microbial community metabolism and host-microbial co-metabolism as a function of diet and microbiome donor.

Transplantation and replication of fecal microbial communities from healthy and kwashiorkor co-twins in gnotobiotic mice

When amplicons were generated from variable region 4 (V4) of bacterial 16S rRNA genes present in the pre-treatment fecal samples of co-twins in discordant pairs and subjected to sequencing with an Illumina HiSeq instrument (403,603±97,345 reads/sample; **table S2A**), we did not find any phylum-, class-, order-, family-, genus or species-level taxa whose proportional representation were significantly different between healthy and kwashiorkor microbiota across *all* twin pairs. In the absence of a distinct and consistent taxonomic signature of kwashiorkor, we selected pre-treatment fecal samples from three discordant twin pairs for microbiota transplants into adult germ-free C57BL/6J mice based on the following criteria: all twin pairs were roughly the same age, and neither co-twin in any pair had diarrhea, vomiting, or were consuming antibiotics at the time that fecal samples were collected. The twins selected included DZ pair 196 (aged 16.5 months), DZ pair 56 (aged 18 months), MZ twin pair 57 (aged 21 months) (see **fig. S4** and **table S2A** for clinical characteristics).

Based on diet surveys of food ingredients and the frequency of their representation (*9*), we constructed a diet that reflected the staple foods consumed by individuals living in rural southern Malawi. The Malawian diet had low caloric density (1.0 kcal/g) and was deficient in multiple micro- and macronutrients as judged by

established nutritional recommendations for mice and for humans aged 1-3 (**table S6**). We also generated the peanut-based RUTF. Both diets were sterilized by irradiation.

Phenotypic effects – Previously frozen, pre-treatment fecal microbiota from the 6 selected human donors were each transplanted, with a single oral gavage, into separate groups of 8 week-old male germ-free C57BL/6J mice. Animals were placed on the Malawi diet beginning one week prior to gavage (n=5 mice cage; 5-10 animals/treatment group; each treatment group maintained in a separate gnotobiotic isolator; diet given *ad libitum*; **fig. S5**). In the case of two of the three discordant twin pairs, transplantation of the kwashiorkor co-twin's microbiota resulted in significantly greater weight loss in recipient mice over the ensuing 3 weeks than those harboring their healthy sibling's microbiota. The discordance in weight loss was greatest for twin pair 196 where recipients of the healthy co-twin's microbiota maintained weight while those that received the kwashiorkor co-twin's microbiota lost 33.9±9.4% of their pre-gavage body mass (**Fig. 2A**). In the case of family 57, mice harboring the kwashiorkor co-twin's microbiota lost 20.0±9.3% of their body mass during this 3-week period, while recipients of microbiota from co-twins belonging to family 56 did not manifest a discordant phenotype (data not shown).

Three weeks after gavage, mice were switched to RUTF. At the time of the diet switch, recipients of kwashiorkor microbiota from families 196 and 57 had become severely anorectic. All mice in each treatment group rapidly gained weight while consuming RUTF. In the case of the most discordant set of recipients (from family 196), mice with the kwashiorkor co-twin's microbiota did not achieve the same body weight as recipients of the healthy sibling's microbiota, but did reach 96.8%±2.8% of their pre-

gavage weight (**Fig. 2A**). After two weeks on RUTF, all mice in all treatment groups were returned to the Malawian diet. While all recipients of microbiota transplants lost weight, this re-exposure did not produce the profound weight loss in mice colonized with the kwashiorkor microbiota that had been documented during their first exposure (**Fig. 2A**). These results indicate that the gut microbiota from two of the three discordant pairs are able to transmit a discordant malnutrition phenotype manifested by weight loss to recipient gnotobiotic mice. Given that the most discordant weight loss phenotype was produced by microbiota from twin pair 196, we initiated an in-depth analysis of their transplanted microbial communities.

The efficiency of transplantation of the kwashiorkor and healthy co-twin microbiota – **Figure S5** shows the time points when samples were collected from gnotobiotic mouse recipients of microbiota transplants from discordant co-twins in family 196. Amplicons were generated from the V4 region of bacterial 16S rRNA present in the input human samples, as well as in the fecal microbiota of all mouse recipients, and sequenced (204,585±181,417 reads/sample; 10 recipients/microbiota; up to 8 time points surveyed/diet/mouse; n=379 samples; **table S2B**). DNA isolated from fecal samples collected at the end of each diet period was also subjected to shotgun pyrosequencing (n=54 samples; **table S2C**). Reads were assigned to KEGG ECs as above.

Transplantation of the human donor microbiomes was quite efficient as judged by the representation of ECs in the input human fecal sample compared to their representation in 'output' fecal samples collected from each mouse in each recipient group three weeks post-gavage while they consumed the Malawian diet (90.6% and 89.6% of the 859 ECs detected in each of the input communities from the healthy and

kwashiorkor co-twin donors, respectively, were identified in the fecal microbiota of transplant recipients). Moreover, the proportional representation of ECs in the fecal communities of the donors was highly correlated with their proportional representation in the fecal microbiota of transplant recipients (R^2=0.893-0.936; **fig. S6A,B**).

Table S7A,B provides species-level data from the V4-16S rRNA datasets generated from the fecal microbiota of mice harboring the transplanted family 196 microbiota. Sixty-two of the 72 species-level taxa present in the input community from the healthy co-twin were detected in fecal microbiota collected from all transplant recipients across time and diets. Fifty-eight of the 67 species level taxa were found in the case of the kwashiorkor co-twin transplant.

We used established PCR-Luminex assays (*16-19*) to test for 22 common bacterial, parasitic, and viral enteropathogens in the input human microbiota as well as in recipient mouse fecal samples. Microbiota of members of this family (and the other discordant pair from family 57) harbored protozoan (*Giardia* and *Cryptosporidium*) as well as bacterial pathogens [*Campylobacter*, atypical enteropathogenic *E. coli* (EPEC), enterotoxigenic *E. coli* (ETEC), and enteroinvasive *E. coli*/*Shigella*]. This diversity and multiplicity of enteropathogens is not surprising in children from low-income countries (*20*). The presence of several enteropathogens appeared to cluster within the families (e.g., *Giardia*, atypical EPEC, ETEC, *Shigella*/EIEC, and *Campylobacter*); however, levels were not significantly different between the healthy and kwashiorkor co-twins (two-way ANOVA with Bonferroni post-test; **fig. S7A**). Atypical EPEC and ETEC, detectable in the fecal microbiota of both co-twins in family 196, were transferred to recipient gnotobiotic mice but cleared rapidly (**fig. S7B**). *Cryptosporidium* DNA was present at

high levels in the kwashiorkor co-twin from family 196 but was only detected at two time points in one of the gnotobiotic recipients (**fig. S7C**). We concluded that the markedly discordant weight loss phenotype in recipients of these microbiota did not simply track with the enteropathogen DNA findings.

The effect of diet on the configuration of transplanted microbiota from family 196 - Comparing the two groups of gnotobiotic transplant recipients on a Malawian diet disclosed significant differences in the proportional representation of 37 species-level taxa. Organisms with the most statistically significant differences, and whose relative proportion were higher in mice with the kwashiorkor microbiota were *Bilophila wadsworthia*, a hydrogen-consuming, sulfite-reducing Proteobacteria related to members of Desulfovibrio, that is associated with appendicitis and inflammatory bowel disease (IBD) in humans, and induces a pro-inflammatory T-helper 1 response in a mouse model of IBD (*21-25*), and *Clostridium innocuum*, a gut symbiont that can function as an opportunist in immunocompromised hosts (*26*) (**table S8B**). *B. wadsworthia* and members of the order Clostridiales were also overrepresented in the fecal microbiota of the kwashiorkor co-twin from family 196 compared to his healthy co-twin at the time he presented with SAM (**table S8B**).

Switching from a Malawian diet to RUTF produced a rapid change in configuration of the fecal microbiota. This change was most pronounced in recipients of the kwashiorkor co-twin's community (see PC1 in the PCoA plot of weighted UniFrac distance measurements in **Fig. 2B** and **fig. S8A,B**). Thirty species-level taxa exhibited significant changes in their representation in kwashiorkor microbiota transplant recipients (**Fig. 2C, tables S7B** and **S8A)** with prominent increases in *Bifidobacteria* (*B.*

longum, *B. bifidum,* plus another unclassified taxon or taxa), two *Lactobacilli* [*L. reuteri* and *L. gasseri*, which can produce bacteriocins and stimulate the innate immune system to inhibit the growth and eliminate various enteropathogens (*27-33*)], plus two members of *Ruminococcus* [*R. torques*, a mucus degrader (*34*), and *Faecalibacterium prausnitzii*, a member of the order Clostridiales that exhibits anti-inflammatory activity in a mouse model of colitis, and whose decreased representation is associated with increased risk of ileal Crohn's disease (*35*)]. There were statistically significant decreases in the representation of members of the Bacteroidales (*B. uniformis, Parabacteroides distasonis*, plus an unclassified *Parabacteroides* taxon or taxa).

The time courses of these responses differed. The bloom in *Lactobacilli* occurred early during treatment with RUTF but regressed by the end of this diet period and remained unchanged when animals returned to the Malawian diet. The *Bifidobacterium* spp also bloomed early during administration of RUTF. Unlike the *Lactobacilli*, their increase was sustained into the early phases of the second Malawian diet period (M2) after which they diminished. Like the members of *Bifidobacterium*, *R. torques* increased its representation during RUTF and then rapidly diminished when mice returned to a Malawian diet. The increase in *F. prausnitzii* was sustained into and through M2. The responses of the Bacteroidales were opposite to that of the other three groups: they decreased with RUTF and re-emerged with M2 (**Fig. 2C**, **tables S7B** and **S8A**).

Twenty-eight bacterial species-level taxa exhibited significant changes in their representation in gnotobiotic mice harboring the healthy co-twin's microbiota in response to RUTF. The response of the *Lactobacilli* observed in the kwashiorkor transplant recipients was not seen in gnotobiotic mice containing the healthy co-twin's

microbiota. The pattern of change of 13 different taxa including the two *Ruminococcus* spp., *B. uniformis*, *P. distasonis, B. longum* and an unclassified *Bifidobacterium* taxon or taxa were shared by both recipient groups (healthy and kwashiorkor), although the *Bifidobacterium* response was more diminutive in the healthy microbiota treatment group (**Fig. 2C, tables S7A** and **S8A,B**). These changes were representative of those that occurred in the human donors: members of *Ruminococcus* increased with RUTF in both co-twins, while the change in *Bifidobacterium* was unique to the kwashiorkor co-twin (**table S9**).

Responses that were specific to mice containing the healthy co-twin's microbiota included increases in *Parabacteroides merdae*, an unclassified taxa or taxon from the genus *Faecalibacterium*, as well as an unclassified taxa or taxon from the family *Coriobacteriaceae* when mice switched to a RUTF diet. Of these, only *Parabacteroides merdae* did not persist when animals were returned to the Malawian diet (**Fig. 2C, table S7A** and **S8A**).

Effect of diet on the metabolic profiles of transplanted kwashiorkor and healthy co-twin microbiomes from family 196 – We performed targeted GC-MS analyses of short chain fatty acids (SCFA), and non-targeted GC-MS of 69 other products of carbohydrate, amino acid, nucleotide and lipid (fatty acid) metabolism in fecal samples collected 10 and 16 days after gavage during the first Malawian diet phase (M1), 2 and 10 days after switching to RUTF, and 26 days after return to the second Malawian diet phase (M2) (n=4-5 mice/family 196 microbiota donor). PCoA plots, based on Hellinger distance measurements of fecal metabolite profiles, revealed a marked effect of RUTF in both groups of mice (see PC1 in **fig. S9A**). PC2 disclosed a donor microbiota effect, with a

prominent difference between recipient groups evident after the switch from RUTF back to a Malawian diet (**fig. S9B**).

Figure S9C displays metabolites that exhibited statistically significant differences in their levels in both groups of transplant recipients when they were consuming RUTF versus the Malawi diet ($p<0.05$; unpaired Student's t-test). Levels of the majority of metabolites, including amino acids, fatty acids, and products of nucleotide metabolism, increased when mice were switched to RUTF. In contrast, levels of several di- and monosaccharides (maltose, gentibiose and tagatose) decreased.

There were a number of significant differences in metabolite levels in feces harvested from mice containing the transplanted kwashiorkor versus healthy co-twin microbiota while they were consuming the different diets (**Fig. 3**). For example, switching to RUTF produced a significant increase in levels of 6 essential amino acids (valine, leucine, isoleucine, methionine, phenylalanine, threonine) and 3 nonessential amino acids (alanine, tyrosine, serine) in both groups of mice (**fig. S10A,B**). However, in the kwashiorkor group, the response was initially greater but subsequently diminished and was surpassed by the increase observed in mice with the healthy co-twin's microbiota. Four weeks after returning to a Malawian diet, levels of 6 of these amino acids remained higher in the healthy microbiota recipient group than before RUTF. In contrast, in the kwashiorkor group they fell to pre-RUTF treatment levels (**fig. S10A,B**). The same pattern of transient response was observed with urea cycle intermediates in the kwashiorkor group (**fig. S10C**). Targeted GC-MS of SCFA showed a significant RUTF-associated increase in levels of propionate, butyrate, lactate and succinate in both groups of mice: this increase was rapid, confined to the early period of RUTF

consumption, and was generally greater in mice harboring the healthy co-twin's microbiota (**fig. S11A**). Acetate levels in the healthy but not the kwashiorkor microbiota group showed the same pattern of change (**fig. S11A**). Increases in these end products of fermentation were accompanied by reductions in the levels of a number of mono- and disaccharides (**fig. S11B**). The observed differences in metabolic profiles were not attributable to differences in microbial community biomass: there were no statistically significant differences in fecal DNA content between the two groups of mice when assayed at the midpoint of RUTF treatment or 4 weeks after cessation of treatment (data not shown).

Procrustes analysis of data obtained from the transplanted microbiota from discordant co-twins in family 196 (**fig. S12**) revealed significant correlation between metabolic and taxonomical profiles on each diet with an overall goodness of fit (M^2 value) of 0.380 ($p<0.0001$; 1,000 Monte Carlo label permutations) for all diets and microbiota.

Shared microbial responses between mice receiving transplants from discordant pairs 196 and 57 – As in the case of discordant twins belonging to family 196, transplantation of fecal microbiota from discordant twin pair 57 was highly efficient. Only 4 of 69 and 2 of 76 species-level taxa detected in the input community were not detected in the output fecal microbiota of healthy and kwashiorkor co-twin microbiota transplant recipients, respectively (**table S7C,D**). Moreover, 87.4-92.3% of the 835 ECs present in the input communities were detected in the recipient mice, and the proportional representation of these ECs in the input and 'output' fecal samples was highly correlated (R^2=0.784-0.859; **fig. S6C,D**).

Thirty-three species-level taxa were identified whose proportional representation was significantly different in the fecal microbiota of the two groups of family 57 transplant recipients when they were consuming a Malawian diet (**table S8D**). Six of these taxa showed corresponding significant differences in recipients of the discordant twin pair 196 microbiota (noted in bold font in **table S8D**). Taxa that showed higher proportional representation in both sets of mice with the kwashiorkor microbiota included *Bilophila wadsworthia*, *Dorea formicigenerans*, a producer of formate used by sulfur-reducing bacteria (*36*), *Coprococcus comes*, a Firmicute associated with Crohn's disease (*37*), plus an unclassified Bacteroidales taxon or taxa. Examining 16S rRNA data generated from the human fecal samples prior to transplantation, we found that as with family 196, *B. wadsworthia*, as well as members of the order Clostridiales (*Coprococcus comes*, *Dorea formicigenerans*), and the order Bacteroidales were overrepresented in the microbiota of the kwashiorkor co-twin in family 57 compared to the well-nourished sibling (**table S8B,D**).

Like family 196 recipient mice, switching from the Malawian diet to RUTF produced a rapid change in microbiota configuration, with the family 57 kwashiorkor microbiota recipients exhibiting a more dramatic change than recipients of the healthy sibling's microbiota (**fig. S8C,D**). Moreover, the kwashiorkor gut community underwent many of the same changes seen with the family 196 kwashiorkor sample, including changes in *Bifidobacterium* (*B. longum*, *B. bifidum* and another unclassified taxa or taxon), *R. torques*, and *Bacteroidales* (*B. uniformis*, *Parabacteroides distasonis* and an unidentified *Parabacteroides* taxa or taxon) (**tables S7D** and **S8C**). **Table S9** compares common changes observed in mice and in twins in families 196 and 57 to changes noted in the

other 11 discordant twin pairs as a function of health status and diet; e.g., *Collinsella aerofaciens, Coprococcus comes, Ruminococcus obeum, Dorea formicigenerans* and *Bifidobacterium longum* showed similar patterns in most twin pairs.

GC-MS of mouse fecal samples, collected on the last day of each diet period, revealed a very similar metabolic profile to that seen in mice who had received transplants from discordant pair 196, with essential and non-essential amino acids, fatty acids, and products of nucleotide metabolism manifesting statistically significant differences in their levels when mice were consuming RUTF versus the Malawian diet (**fig. S13,** $p<0.05$; unpaired Student's t-test).

Microbial-host co-metabolism as a function of donor microbiota and host diet

Untargeted urine metabolite profiles were obtained from mice that were the recipients of microbiota transplants from discordant twin pairs using standard ^{1}H NMR spectroscopic analysis (*38*). The initial global metabolite profiles from samples obtained during the M1 diet period were significantly different between mice transplanted with the kwashiorkor versus the healthy co-twin microbiota. For discordant twin pair 196, the kwashiorkor microbiota was associated with higher levels of urinary allantoin (an end product of purine metabolism in non-primates, equivalent to uric acid in humans), creatine and creatinine (markers of muscle turnover), and dimethylamine (linked to gut microbial metabolism of choline via trimethylamine). Lower urinary concentrations of 2-oxoadipate (a product of lysine metabolism) and trimethylamine (from choline) were also noted (**table S10**). Mice harboring transplanted microbiota from kwashiorkor co-twin 57 also showed increased urinary excretion of allantoin, creatine and dimethylamine. Increased excretion of phenylacetylglycine (microbial-host co-

metabolite from colonic phenylalanine metabolism), trimethylamine-*N*-oxide (alternative metabolic product of trimethylamine derived from choline), and acetate were characteristic for mice harboring the microbiota for kwashiorkor co-twin 57; these latter differences were not significant in recipients of the discordant family 196 twin microbiota although there was a trend towards increased trimethylamine-*N*-oxide excretion in mice harboring the kwashiorkor community.

Levels of urinary taurine were affected by both donor microbiota and diet. Mice harboring a healthy donor microbiota excreted more taurine while consuming both the Malawian diet and RUTF compared to mice with a kwashiorkor microbiota; in both groups, urinary taurine levels were higher when mice were consuming a Malawian diet (**table S10**). *B. wadsworthia* grows well on bile acids and uses taurine from taurine-conjugated bile acids as a terminal electron acceptor, converting it to ammonia, acetate and sulfide (*39*). In agreement with this property, fecal levels of *B. wadsworthia* showed an inverse relationship with urinary taurine levels, falling in mice harboring the kwashiorkor co-twin microbiota from 5.1% during the M1 diet phase to 1.9% on RUTF and rising to 2.1% during the M2 diet period; in contrast, levels remained <0.1% in mice with the healthy sibling's microbiota (**table S8A,B**).

Figure 4A shows how RUTF had a dominant effect on metabotype as evidenced by the apparent clustering of urine samples from mice colonized with microbial communities from the family 196 twin pair, whereas urine samples from the healthy and kwashiorkor groups showed a clear distinction when mice were consuming the Malawian diet. However, a separate PCA model of urine samples obtained during the

RUTF dietary period (**Fig. 4B**) reveals differences between healthy and kwashiorkor microbiota transplant recipients.

The pronounced metabolic shift in response to the RUTF diet was not sustained on re-introduction of the Malawian diet; metabolic profiles at the end of the M2 period resembled those from M1, with renewed differentiation of the healthy versus kwashiorkor microbiota transplant groups, although the kwashiorkor microbiota-associated metabolic phenotype was not as distinctive as with M1 (**Fig. 4C**). When the data were remodeled excluding the RUTF samples, metabolic differentiation was more apparent between the two Malawian dietary periods and between mice harboring the healthy versus kwashiorkor co-twin microbiota, with relatively greater differentiation observed between healthy and kwashiorkor in M1 (**Fig. 4C**).

Differences between healthy and kwashiorkor microbiota from discordant twin pair 196 were also observed in the plasma metabolome (**Fig. 4D**) with higher glucose concentrations and lower levels of citrate, acetate, lactate and tyrosine in mice harboring the healthy co-twin's microbiota.

In the case of mice containing the healthy co-twin's microbiota, the urinary excretion behaviors of the tricarboxylic acid (TCA) cycle intermediates 2-oxoglutarate, citrate, succinate and fumarate were closely coupled together when mice were compared during the M1 versus RUTF, RUTF versus M2, and M1 versus M2 diet periods. Similarly, they were closely coupled when healthy versus kwashiorkor transplant recipients were compared during the M1 or RUTF or M2 periods (**table S10**). It is known that these mitochondrial metabolites typically follow similar reabsorption control mechanisms in the renal tubule that are closely linked to tubular pH. Under conditions

of renal tubular acidosis, renal mitochondria utilize the intermediates at a higher rate and, consequently, a greater proportion of these intermediates are reabsorbed from the urine, driven by the concentration gradient. In mice colonized with the kwashiorkor but not the healthy microbiota, fumarate excretion was effectively decoupled from the other TCA intermediates (**table S10**). Such differential excretion rates of TCA intermediates can occur where there is selective enzymatic inhibition of the TCA cycle (*40*). There also appears to be a disruption in the TCA cycle in the microbiota with significantly increased levels of succinate (3-fold, $p<0.05$, unpaired Student's t-test), and an increased succinate to fumarate ratio (0.58 versus 0.23, $p<0.05$, unpaired Student's t-test) in cecal samples from the kwashiorkor recipient mice, suggesting inhibition of succinate dehydrogenase, the enzyme responsible for converting succinate to fumarate. Taken together, these observations suggest that the kwashiorkor microbiota examined in these gnotobiotic mice may generate chemical products that result in a selective inhibition of one or more TCA cycle enzymes, with concomitant effects on host energy metabolism. This hypothesis warrants further study, first in humanized gnotobiotic mice and subsequently in discordant twins.

Prospectus

The observation that discordance rate for kwashiorkor is so high in twins in our study population, and that no statistically significant difference exists in discordance rates between mono- versus dizygotic twins, focuses attention on the need to delineate the impact of environmental exposures on the pathogenesis of this enigmatic disease: this includes a systematic analysis of maternal and infant characteristics. Our results illustrate the value of studies using twins discordant for nutritional phenotypes to

characterize the interrelationship between the functional development of the gut microbiota in children and their nutritional status. Linking metagenomic analyses of the compositional features of these communities to their subsequent transplantation and replication in groups of gnotobiotic mice who are fed diets representative of those consumed by the human microbiota donors, has provided evidence that the microbiota is likely a causal factor in the pathogenesis of kwashiorkor. By replicating a human donor's microbiota in multiple recipient gnotobiotic mice and subjecting the mice to the same therapeutic dietary manipulations as those experienced by human donors, but under more controlled conditions, we have been able to mimic a clinical intervention, identify community characteristics, including differences in taxonomic composition and differences in taxonomic and metabolic responses to RUTF, that are informative at several levels. *First*, they provide biomarkers of community metabolism and of microbial-host co-metabolism that delineate and discriminate diet and microbiota effects, including biomarkers indicative of the more labile, short-lived nature of the responses of microbiota from kwashiorkor donors to RUTF. These discriminatory biomarkers can serve as the basis for more detailed studies of microbiota samples obtained from the human donors used to create the mouse model, as well as larger population studies. *Second*, these mice provide insights about pathogenesis by identifying transmissible features of the community, including those that are diet-associated, thereby distinguishing casual versus causal relationships between microbiota and human host phenotypes. Although beyond the scope of the present study, the interrelationships between diet, microbiota, and many facets of host physiology can be explored in detail in these 'personalized' gnotobiotic mouse models, such as how the combination of a given diet and microbiota influences functional properties of the innate

and adaptive arms of the immune system, overall energy homeostasis, or neurologic functions. *Third*, these models may not only provide a way for identifying different pathogenetic mechanisms and distinguishing disease subgroups, but also for developing new and more effective approaches for treatment and/or prevention. On the one hand, the effects of different therapeutic diets, formulated based on metabolic deficiencies observed in these gnotobiotic mouse models, can be systematically evaluated, including whether their long-term administration can repair metabolic dysfunctions associated with the gut communities from malnourished individuals, whether their effects are generalizable to microbiota transplanted from donors representing different geographic locations, and whether the reconfiguration of community properties they produce can be sustained after withdrawal of treatment. On the other hand, these models can help identify lead probiotic species, especially given recent advances that allow an extensive culture collection to be generated from an intact uncultured microbiota once that microbiota is observed to transmit a phenotype to recipient mice (*15*). In addition, characterization of microbial-host co-metabolism can yield testable hypotheses about potential host therapeutic targets. For example, an intriguing hypothesis, based on measurements of cecal and urinary levels of TCA cycle intermediates is that a kwashiorkor microbiota, when exposed to a Malawi diet, may produce one or more inhibitors of mitochondrial TCA cycle enzymes, making energy metabolism a bigger challenge for these children when they are exposed to a micro- and macronutrient deficient, low calorie diet. Finally, studies of other forms of malnutrition using an approach analogous to that described in this study, could also help provide insights about the contribution of gut microbiota to this devastating global health problem.

References:

1. UN Inter-Agency Group for Child Mortality Estimation (UNIGME), *Levels & Trends in Child Mortality Report*. (2011; www.childinfo.org/files/Child_Mortality_Report_2011.pdf).

2. World Health Organization Multicentre Growth Reference Study Group (WHO MGRSG), WHO child growth standards based on length/height, weight and age. *Acta Paediatr.* **Suppl. 450**, 76-85 (2006).

3. C. D. Williams, B. M. Oxon, H. Lond, Kwashiorkor: a nutritional disease of children associated with a maize diet. *Lancet* **226**, 1151-1152 (1935).

4. T. Ahmed, S. Rahman, A. Cravioto, Oedematous malnutrition. *Indian J. Med. Res.* **130**, 651-654 (2009).

5. C. Gopalan, in *Calorie Deficiencies and Protein Deficiencies: Kwashiorkor and marasmus: evolution and distinguishing features*, R. A. McCance, E. M. Widdowson, Eds. (Churchill London, UK, 1968), pp. 48-58.

6. M. H. Golden, Protein deficiency, energy deficiency, and the oedema of malnutrition. *Lancet* **1**, 1261-1265 (1982).

7. M. H. Golden, The development of concepts of malnutrition. *J. Nutrition* **132**, 2117S-2122S (2002).

8. C.A. Lin *et al.*, A prospective assessment of food and nutrient intake in a population of Malawian children at risk for kwashiorkor. *J. Pediatr. Gastroenterol. Nutr.* **44**, 487-493 (2007).

9. T. Yatsunenko *et al.*, Human gut microbiome viewed across age and geography. *Nature* **486**, 222-227 (2012).

10. R. E. Black *et al.*, Maternal and child undernutrition: global and regional exposures and health consequences. *Lancet* **371**, 243-260 (2008).

11. World Health Organization, World Food Programme, United Nations System Standing Committee on Nutrition, United Nations Children's Fund, Community-Based Management of Severe Acute Malnutrition, *Community-based management of severe acute malnutrition* (2007; www.who.int/nutrition/topics/statement_commbased_malnutrition/en/index.html).

12. World Health Organization, United Nations Children's Fund, WHO Child Growth Standards and the Identification of Severe Acute Malnutrition in Infants and Children. *WHO child growth standards and the identification of severe acute malnutrition in infants and children* (2009; www.who.int/nutrition/publications/severemalnutrition/9789241598163/en/index.html).

13. L. LaGrone, S. Cole, A. Schondelmeyer, K. Maleta, M. J. Manary, Locally produced ready-to-use supplementary food is an effective treatment of moderate acute malnutrition in an operational setting. *Ann. Trop. Paed.* **30**, 103-108 (2010).

14. P. J. Turnbaugh *et al.*, The effect of diet on the human gut microbiome: a metagenomic analysis in humanized gnotobiotic mice. *Sci. Transl. Med.* **1**, 6ra14 (2009).

15. A. L. Goodman, G. Kallstrom, J. J. Faith, A. Reyes, A. Moore, G. Dantas, J. I. Gordon, Extensive personal human gut microbiota culture collections characterized and manipulated in gnotobiotic mice. *Proc. Natl. Acad. Sci. U. S. A*. **108**, 6252-6257 (2011).

16. J. Liu *et al.*, Simultaneous detection of six diarrhea-causing bacterial pathogens with an in-house PCR-luminex assay. *J. Clin. Microbiol*. **50**, 98-103 (2012).

17. M. Taniuchi *et al.*, Multiplex polymerase chain reaction method to detect Cyclospora, Cystoisospora, and Microsporidia in stool samples. *Diagn. Microbiol. Infect. Dis*. **71**, 386-390 (2011).

18. M. Taniuchi *et al.*, High throughput multiplex PCR and probe-based detection with Luminex beads for seven intestinal parasites. *Am. J. Trop. Med. Hyg*. **84**, 332-337 (2011).

19. M. Taniuchi *et al.*, Development of a multiplex polymerase chain reaction assay for diarrheagenic Escherichia coli and Shigella spp. and its evaluation on colonies, culture broths, and stool. *Diagn. Microbiol. Infect .Dis.* **73**, 121-128 (2012).

20. M. J. Albert, A. S. Faruque, S. M. Faruque, R. B. Sack, D. Mahalanabis, Case-control study of enteropathogens associated with childhood diarrhea in Dhaka, Bangladesh. *J. Clin. Microbiol*. **37**, 3458-3464 (1999).

21. E. J. Baron *et al.*, Bilophila wadsworthia, gen. nov. and sp. nov., a unique gram-negative anaerobic rod recovered from appendicitis specimens and human faeces. *J. Gen. Microbiol.* **135**, 3405–3411 (1989).

22. S. M. da Silva, S. S. Venceslau, C. L. Fernandes, F. M. Valente, I. A. Pereira, Hydrogen as an energy source for the human pathogen Bilophila wadsworthia. *Antonie Van Leeuwenhoek*. **93**, 381-390 (2008).

23. W. E. W. Roediger, J. Moore, W. Babidge, Colonic sulfide in pathogenesis and treatment of ulcerative colitis. *Dig. Dis. Sci.* **42**, 1571–1579 (1997).

24. M. Campieri, P. Gionchetti, Bacteria as the cause of ulcerative colitis. *Gut* **48**, 132–135 (2001).

25. S. Devkota *et al.*, Dietary-fat-induced taurocholic acid promotes pathobiont expansion and colitis in Il10(-/-) mice. *Nature* **487**, 104-108 (2012).

26. N. Crum-Cianflone, Clostridium innocuum Bacteremia in a patient with acquired immunodeficiency syndrome. *Am. J. Med. Sci*. **337**, 480-482 (2009).

27. S. E. Jones, J. Versalovic, Probiotic Lactobacillus reuteri biofilms produce antimicrobial and anti-inflammatory factors. *BMC Microbiol*. **9**, 35-43 (2009).

28. A. V. Shornikova, I. A. Casas, E. Isolauri, H. Mykkänen, T. Vesikari. Lactobacillus reuteri as a therapeutic agent in acute diarrhea in young children. *J. Pediatr. Gastroenterol. Nutr*. **24**, 399-404 (1997).

29. T. Itoh, Y. Fujimoto, Y. Kawai, T. Toba, T. Saito, Inhibition of food-borne pathogenic bacteria by bacteriocins from Lactobacillus gasseri. *Lett. Appl. Microbiol*. **21**, 137-141 (1995).

30. I. Sakamoto *et al.*, Suppressive effect of Lactobacillus gasseri OLL 2716 (LG21) on Helicobacter pylori infection in humans. *J. Antimicrob. Chemother*. **47**, 709-10 (2001).

31. A. Ushiyama *et al.*, Lactobacillus gasseri OLL2716 as a probiotic in clarithromycin-resistant Helicobacter pylori infection. *J. Gastroenterol. Hepatol*. **18**, 986-991 (2003).

32. M. F. Fernández, S. Boris, C. Barbés, Probiotic properties of human lactobacilli strains to be used in the gastrointestinal tract. *J. Appl. Microbiol.* **94**, 449-55 (2003).

33. Y. Kato-Mori *et al.,* Fermentation metabolites from Lactobacillus gasseri and Propionibacterium freudenreichii exert bacteriocidal effects in mice. *J. Med. Food* **13**, 1460-1467 (2010).

34. A. A. Salyers, S. E. West, J. R. Vercellotti, T. D. Wilkins, Fermentation of mucins and plant polysaccharides by anaerobic bacteria from the human colon. *Appl. Environ. Microbiol.* **34**, 529-33 (1977).

35. H. Sokol *et al.,* Faecalibacterium prausnitzii is an anti-inflammatory commensal bacterium identified by gut microbiota analysis of Crohn's disease patients. *Proc. Natl. Acad. Sci. U.S.A.* **105**, 16731-16736 (2008).

36. D. Taras, R. Simmering, M. D. Collins, P. A. Lawson, M. Blaut. Reclassification of Eubacterium formicigenerans Holdeman and Moore 1974 as Dorea formicigenerans

gen. nov., comb. nov., and description of Dorea longicatena sp. nov., isolated from human faeces. *Int. J. Syst. Evol. Microbiol*. **52**, 423-428 (2002).

37. F. Wensinck, J. P. van de Merwe, J. F. Mayberry. An international study of agglutinins to Eubacterium, Peptostreptococcus and Coprococcus species in Crohn's disease, ulcerative colitis and control subjects. *Digestion* **27**, 63-69 (1983).

38. O. Beckonert *et al.*, Metabolic profiling, metabolomic and metabonomic procedures for NMR spectroscopy of urine, plasma, serum and tissue extracts. *Nature Protoc.* **2**, 2692-2703 (2007).

39. H. Laue, K. Denger, A.M. Cook, Taurine reduction in anaerobic respiration of Bilophila wadsworthia RZATAU. *Appl. Environ. Microbiol*. **63**, 2016-2021 (1997).

40. J. K. Nicholson, J. A. Timbrell, P. J. Sadler, Proton NMR spectra of urine as indicators of renal damage. Mercury-induced nephrotoxicity in rats. *Mol. Pharmacol.* **27**, 644-651 (1985).

41. M. J. Manary, Local production and provision of ready-to-use therapeutic food (RUTF) spread for the treatment of severe childhood malnutrition. *Food Nutr. Bull.* **27** (3 Suppl), S83-S89 (2006).

42. M. S. McPeek, L. Sun, Statistical tests for detection of misspecified relationships by use of genome-screen data. *Am. J. Hum. Genet*. **66**, 1076-1094 (2000).

43. P. J. Turnbaugh *et al.*, A core gut microbiome in obese and lean twins. *Nature* **457**, 480-484 (2009).

44. J.G. Caporaso *et al.,* Ultra-high-throughput microbial community analysis on the Illumina HiSeq and MiSeq platforms. *ISME J.* **6**, 1621–1624 (2012).

45. J. G. Caporaso *et al.*, QIIME allows analysis of high-throughput community sequencing data. *Nature Methods* **7**, 335-336 (2010).

46. T. K. Teal, T. M. Schmidt, Identifying and removing artificial replicates from 454 pyrosequencing data. *Cold Spring Harbor Protocols,* **4**, (2010), doi:10.1101/pdb.prot5409.

47. F. E. Rey *et al.*, Dissecting the in vivo metabolic potential of two human gut acetogens. *J. Biol. Chem.* **285**, 22082–22090 (2010).

48. J. Pinheiro, D. Bates, S. DebRoy, D. Sarkar and the R Development Core Team (2012). nlme: Linear and Nonlinear Mixed Effects Models. R package version 3.1-104 (2012).

49. N. P. McNulty *et al.*, The impact of a consortium of fermented milk strains on the gut microbiome of gnotobiotic mice and monozygotic twins. *Science Transl. Med.* **3**, 106ra106 (2011).

50. K. A. Veselkov *et al.*, Recursive segment-wise peak alignment of biological ^{1}H NMR spectra for improved metabolic biomarker recovery. *Anal. Chem.* **81**, 56-66 (2009).

51. Subcommittee on Laboratory Animal Nutrition, Committee on Animal Nutrition, Board on Agriculture, National Research Council, *Nutrient Requirements of Laboratory Animals, Fourth Revised Edition, 1995*. (The National Academies Press, ed. 4, 1995).

52. C. M. Chaparro, K. G. Dewey, Use of lipid-based nutrient supplements (LNS) to improve the nutrient adequacy of general food distribution rations for vulnerable sub-groups in emergency settings. *Matern. Child Nutr.* **6**, Suppl 1:1-69 (2010).

Acknowledgements:

We thank Sabrina Wagoner, Jill Manchester and Marty Meier for superb technical assistance; Jill Manchester, Su Deng and Jessica Hoisington-López for assistance with DNA sequencing; Maria Karlsson, David O'Donnell and Sabrina Wagoner for help with gnotobiotic mouse husbandry; Barbara Mickelson from Teklad Diets and Heidi Sandige for assistance with the design of the mouse diets; and members of the Gordon lab for valuable suggestions during the course of this work. This work was supported by grants from the Bill and Melinda Gates Foundation, and the NIH (DK30292, DK078669, T32-HD049338). M.I.S was the recipient of a post-doctoral fellowship from the St. Louis Children's Discovery Institute (MD112009-201). J.V.L was the recipient of an Imperial College Junior Research Fellowship.

Author contributions:

M.I.S., T.Y., and J.I.G designed the experiments; M.M. designed and implemented the clinical monitoring and sampling for the trial, R.M. and I.T. participated in patient recruitment, sample collection, sample preservation and clinical evaluations; M.I.S. performed experiments involving gnotobiotic mice while T.Y. characterized microbiota obtained from twins; M.I.S., T.Y., J.C., S.S.R., P.C., J.C.M., J.L., E.H., J.V.L., E.H., and J.N.

generated data; M.I.S., T.Y., E.H., J.N., D.K, L.K.U, R.K. and J.I.G. analyzed the results; M.I.S., T.Y., and J.I.G. wrote the paper.

Datasets

Illumina V4-16S rRNA and 454 shotgun pyrosequencing datasets have been deposited in EBI.

Figure #:

Fig 1. Functional maturation of the gut microbiomes of Malawian twin pairs concordant for healthy status, and twin pairs who became discordant for kwashiorkor. (**A**) PCoA of Hellinger distances between KEGG EC profiles. The position of each fecal microbiome along principal coordinate 1 (PC1), which describes the largest amount of variation in this dataset of 308 sequenced twin fecal microbiomes, is plotted against age. Each sphere represents a microbiome colored by the age of the human donor. (**B**) Average ± SEM PC1 coordinate obtained from the data shown in panel A for microbiomes sampled at 3 consecutive time points from 9 twin pairs who remained well-nourished (healthy) during the study. (**C**) Average ± SEM PC1 coordinate obtained from panel A for microbiomes sampled before, during and after RUTF treatment from co-twins discordant for kwashiorkor. *$p<0.05$, Friedman test with Dunn's post-hoc test applied to data shown in panels **B** and **C**. [See **fig. S3** which shows how changes in the relative proportion of Actinobacteria parallel the patterns observed with the changes along PC1; children with kwashiorkor manifested a statistically significant decrease in Actinobacteria with introduction of RUTF, unlike their healthy co-twins ($p<0.05$ after FDR correction for comparison of other bacterial phyla].

Fig 2. Transplantation of fecal microbiota from kwashiorkor and healthy co-twins from family 196 into gnotobiotic mice fed Malawian and RUTF diets. (**A**) Discordant weight loss phenotype of recipient mice, n=10 mice/group, *$p<0.05$, Student's t-test. Data points are colored by recipient group; blue, kwashiorkor co-twin fecal microbiota recipients; red, healthy co-twin fecal microbiota recipients. (**B**) Average ± SEM PC1 coordinate obtained from the weighted UniFrac distances shown in **fig. S8A** for fecal

microbiota sampled from mice over time. Same color key as in panel A. (**C**) Heatmap of species-level taxa whose representation in the fecal microbiota of gnotobiotic mice change significantly ($p<0.05$, Students t-test with Bonferonni correction) as a function of donor microbiota and Malawian versus RUTF diets. An asterisk indicates taxa that changed significantly in both groups of microbiota transplant recipients. Species level taxa are colored by phylum; Firmicutes (red), Actinobacteria (blue), Bacteroidetes (black) and Proteobacteria (green).

Fig. 3. Metabolites with significant differences in their fecal levels in gnotobiotic mice colonized with microbiota from discordant twin pair 196 as a function of diet. Data are from fecal samples collected 3 days before the end of (**A**) the first period of consumption of the Malawian diet (M1, day 16; abbreviated M1.D16), (**B**) RUTF treatment (RUTF.D10), (**C**) the second period of Malawian diet consumption (M2.D26). Significant differences are defined as $p<0.05$ according to Student's t-test.

Fig. 4. Principal component analysis (PCA) scores plots derived from ^{1}H-NMR analysis of urine obtained from mice with microbiota transplants from discordant twin pair 196. (**A**) PCA plot of all urine samples from both groups of mice over the three dietary periods emphasizing the impact of RUTF. (**B**) PCA plot of samples collected during the RUTF phase, emphasizing differences between mice harboring healthy and kwashiorkor co-twin microbiota. (**C**) PCA plot excluding samples collected during the RUTF phase, emphasizing differences between mice harboring healthy and kwashiorkor co-twin microbiota and between the two Malawian diet periods. (**D**) PCA lot of plasma samples collected at the end of the second Malawi diet (M2) phase, showing the difference in plasma metabolite profiles between mice harboring healthy (filled squares)

and kwashiorkor (open squares) co-twin microbiota. All datasets were aligned, normalized to total area, centered and log 2 transformed with an offset of 1.

Supplementary Material:

Materials and Methods

Figs. S1-S13

Tables S1-S9

References (*41-52*)

Materials and Methods

Studies in humans

Enrollment, clinical data and sample collection - Subjects were recruited for the present study using procedures approved by the College of Medicine Research Ethics Committee of the University of Malawi, and by the Human Research Protection Office of Washington University in St. Louis. Twin pairs were recruited through health centers located in five rural southern Malawian villages. A team of one USA pediatrician and a minimum of two trained local personnel visited each site every month where the weight and height of each infant or child was measured in three replicates, and each child was checked for bilateral pitting edema. RUTF was produced in Malawi (*41*). On average, twin pairs where one or both co-twins developed kwashiorkor received 9±8 (mean ± SD) weeks of RUTF treatment, while those with marasmus were treated for 11±8 weeks.

During each visit for a scheduled fecal sample collection, each child wore a commercial disposable diaper lined with plastic. Each fecal specimen was frozen within 10 min after it was produced in a cryogenic storage container filled with liquid nitrogen. All samples were subsequently stored at -80^{o}C prior to analyses.

Zygosity tests - Buccal smears were collected using Oragene kits. We selected 48 autosomal SNPs with high heterozygosity in the Yoruban HapMap sample (n=90) from the Illumina DNA Test Panel of 360 SNP loci that have been optimized for the BeadExpress. The SNP minor allele frequencies in Yorubans ranged from 0.28-0.43, and each autosome was sampled by at least one marker (with the exception of 7,19 and 21), with a minimum marker separation of 3Mb. We ran PREST [Pedigree Relationship

Statistical Test (*42*)] to estimate the identity-by-descent sharing and kinship between the relative pairs, and compared reported relationships versus the inferred relationships from the genetic data.

Isolation and sequencing of fecal microbial community DNA - Fecal samples from humans were pulverized with a mortar and pestle in liquid nitrogen. DNA was extracted from aliquots of the pulverized material (*43*). Amplicons, generated by PCR of bacterial 16S rRNA genes present in the fecal DNA samples were subjected to multiplex sequencing with an Illumina HiSeq instrument using procedures described in a previous publication (*44*). Multiplex shotgun 454 Titanium FLX pyrosequencing of each fecal community DNA sample was conducted according to ref. (*9*).

Analysis of metagenomic datasets

16S rRNA – We used QIIME (*45*) to cluster V4-16S rRNA Illumina reads at 97% nucleotide sequence identity (%ID). Closed-reference OTU picking protocol with uclust against the Greengenes database was employed. Reads that did not match the database were excluded from further analyses. Of the 110,819,831 Illumina reads that passed QIIME's quality filters, 93.5% (103,583,462) hit a reference sequence at greater than or equal to 97% ID. Taxonomy was assigned using RDP classifier 2.4. UniFrac distances between samples were calculated using a *de novo* tree constructed from representative sequences defining each OTU. A table of OTU counts per sample was generated and used in combination with the tree to calculate beta diversity. To generate UniFrac distance matrices, all communities were rarefied to 116,440 V4-16S rRNA reads/sample. Unweighted UniFrac rather than weighted UniFrac was used for our analyses due to the

large differences in taxonomic representation among the samples. Nonetheless, the patterns were similar with weighted UniFrac (data not shown).

Shotgun sequences from fecal microbiomes - Shotgun reads produced by 454 Titanium shotgun sequencing were filtered using custom Perl scripts and publicly available software to remove (i) all reads <60 nt, (ii) reads with two continuous and/or three total degenerate bases (N), (iii) all duplicates (a known artifact of pyrosequencing), defined as sequences whose initial 20 nucleotides are identical and that share an overall identity of >97% throughout the length of the shortest read (*46*); and (iv) all sequences with significant similarity to human or mouse reference genomes (Blastn e-value threshold $\leq 10^{-5}$, bitscore ≥ 50, percent identity $\geq 75\%$). In addition, searches against a database of the 462 human gut bacterial genomes (listed in the **table S3**) were conducted with megablast. A sequence read was annotated as the best hit to this database if the E-value was $\leq 10^{-20}$, and at least 90% identical between query and subject. The relative abundances of reads that mapped to each of the 462 genomes were adjusted to genome sizes. For sequences that mapped to more than one genome, counts were adjusted according to unique matches using a previously described procedure (*47*): for example, in the case of a non-unique read that equally matched genome A and genome B, and where two unique reads matched genome A and eight unique reads matched genome B, 0.2 counts would be assigned to genome A and 0.8 counts to genome B.

Searches against protein-coding component of the KEGG database (version 58) were conducted with BLASTX. Counts were normalized to the mapped reads. 26±4% of the reads mapped to KEGG ECs and 55±14% to the 462 reference human gut genomes. Unmapped reads were excluded from the analyses shown, although repeating the

analyses including these reads had little effect on the results. To quantify the differences in KEGG EC profiles among fecal microbiomes, evenly rarefied matrices of EC counts were created with all samples, and Hellinger distances were calculated using QIIME. T-test and linear mixed-effects regression analyses were conducted in R statistical software using package NLME (*48*) for the latter analysis.

Studies in gnotobiotic mice

Colonization of germ-free animals

All experiments involving mice were performed using protocols approved by the Washington University in St. Louis Animal Studies Committee. Germ-free 8 week-old, male C57BL/6J mice were maintained in flexible plastic gnotobiotic isolators (Class Biologically Clean Ltd., Madison, WI) under a strict 12-hour light cycle (lights on at 0600h) and fed *ad libitum*. Transplantation of human fecal microbiota was performed by first pulverizing the frozen fecal sample with mortar and pestle in liquid nitrogen. Approximately 200 mg of the pulverized sample was diluted in 4 mL of sterile PBS/2mM DTT at room temperature in an anaerobic chamber (Coy Lab Products, Grass Lake, MI; atmosphere composed of 75% N_2/20% CO_2/5% H_2). The fecal material was suspended by vortexing (3 min at room temperature) and the resulting suspension was allowed to settle by gravity (2 min at room temperature in the anaerobic chamber). The supernatant was placed in a sterile polypropylene tube that was capped and placed in a Balch tube. The Balch tube was then capped, taken out of the Coy chamber and transported, at room temperature, to our gnotobiotic mouse facility (~10 minute-long trip). The polypropylene tube was then removed from the protective Balch tube, placed in a transfer sleeve attached to the gnotobiotic isolator and its external surface was

sterilized during a 20 min exposure to 2% chlorine dioxide. Once introduced into the gnotobiotic isolator, the tube was opened, and a ~200 μL aliquot was gavaged, using a flexible plastic tube attached to a sterile syringe, directly into the stomach of each germ-free recipient mouse (n=5-10 mice per donor microbiota preparation).

All mice that received a fecal microbiota sample from a given human donor were co-housed (n=5/cage) in a given gnotobiotic isolator. Different isolators were used for different donors. The sterility of germ-free mice and their isolators was established by routine culture-based surveys of fecal samples as well as by PCR of fecal DNA using universal bacterial 16S rRNA primers.

Preparation of human diets given to gnotobiotic mice

Ingredients for constructing a representative Malawi diet, and the peanut-based RUTF, were purchased from vendors in the USA. Meseca® instant corn flour was obtained from Restaurant Depot (College Point, NY). Organic mustard greens, yellow onions and vine-ripened tomatoes were purchased fresh from Whole Foods Supermarkets. Ground peanuts were from East Wind Nut Butters (Tecumseh, MO).

Food was prepared in 18 kg batches. Four kilograms of corn flour were added to 12.3 liters of freshly autoclaved water and blended for 5 min using an industrial mixer (Globe SP30P 30-quart pizza mixer; gear speed 1; Globe Food Equipment Company, Dayton, OH). This step was followed by addition of 1.63 kg of a relish. This relish was produced by adding 770 g of mustard greens to 154 g of yellow peeled onions, 385 g of vine-ripened tomatoes and 321 mL of water. The mixture was then pureed for 10 min in a vertical cutter mixer (Robot Coupe Model R23, Jackson, MS) and simmered for 30 min

on a Corning stirrer/hot plate (high setting) prior to addition to the corn-water solution. Following addition of the relish, food was blended in the mixer for 5 min. Two to three batches of food were prepared in succession over the course of a day, with each batch being temporarily stored in covered plastic containers. At the end of the day, subsets of each batch were mixed together so that there was a homogeneous product. The finished product was then vacuumed packed in 500 g aliquots in FDA/USDA-compliant poly-nylon vacuum pouches, double-bagged, and sterilized by irradiation (20-50 kGy) within 24 h of its production (Steris Co; Chicago, IL). The macro- and micronutrient content of the cooked and irradiated Malawian diet was defined by N.P. Analytical Laboratories (St Louis, MO) (**table S6**). Food was stored at 4^{o}C for up to six months. Sterility was verified using the same culture methods employed to survey gnotobiotic isolators (see above).

Peanut-based RUTF was produced by Harlan Laboratories (Madison, WI) using a recipe described in a previous publication (*41*). RUTF was packaged and sterilized as above.

Plastic bags containing 500 g of a given diet were introduced into each gnotobiotic isolator after sterilizing the external surface with 2% chlorine dioxide. A small incision was placed at one corner of each bag so that the food, which had the consistency of paste, could be extruded into sterilize glass petri dishes placed in two locations in each cage. Food was refreshed twice per day, allowing for *ad libitum* feeding.

Sample collection

Fecal samples collected from mice were frozen and stored -80°C within 30 min of their production. Fecal and urine samples collected for metabolomic analyses were frozen in liquid nitrogen within 2-10 min after they were produced and subsequently stored at -80°C. Just prior to sacrifice, blood was obtained by retro-orbital phlebotomy.

Isolation and sequencing of fecal DNA

Isolation of fecal DNA, bacterial V4-16S rRNA amplicon and whole community shotgun sequencing, and analyses of the resulting datasets were conducted as described above for human samples.

qPCR assays for enteropathogens

DNA isolated from human donor fecal samples and mouse fecal pellets was tested for 22 enteropathogens using a custom, multiplex, reverse transcription PCR Luminex assay (*16-19*) for detecting Adenovirus, *Ancylostoma duodenale*, *Ascaris lumbricoides*, *Campylobacter jejuni/coli*, *Cryptosporidium* spp., *Cyclospora cayetanensis*, *Cystoisospora belli*, *Enterocytozoon bieneusi*, *Encelphalitozoon intestinalis*, enteroaggregative *E. coli* (EAEC), enterohemorrhagic *E. coli* (EHEC), enteropathogenic *E. coli* (EPEC), enterotoxigenic *E. coli* (ETEC), enteroinvasive *E. coli* (EIEC)/*Shigella* spp., *Entamoeba histolytica*, *Giardia lamblia*, *Necator americanus*, *Salmonella* spp., *Strongyloides stercoralis*, *Trichuris trichiura*, *Vibrio cholera/parahaemolyticus* and *Yersinia* spp. Atypical EPEC was inferred if *eae* was present without *bfpa* (characteristic of typical EPEC) or *stx1/stx2* (present with EHEC). Our assay for the heat-stable enterotoxin of ETEC detects *STh*, while *ipaH* detects but does not discriminate between enteroinvasive *E. coli* (EIEC) and *Shigella* spp.

Metabolomic analyses

Targeted gas chromatography-mass spectrometry - Fecal pellets were weighed in 2 mL polytetrafluoroethylene (PFTE) screw cap vials. A mix of internal standards (20µM of acetic acid-$^{13}C_2$,d_4, propionic acid-d_6, butyric acid-$^{13}C_4$, lactic acid-3,3,3-d_3 and succinic acid-$^{13}C_4$ in a volume of 10 µL) was added to each vial, followed by 20 µL of 33% HCl. Diethyl ether (1mL) was introduced and the mixture vortexed vigorously for 10 min. The two phases were separated by centrifugation (4,000 x g for 5 min at room temperature). The upper organic layer was transferred into another clear vial and a second diethyl ether extraction was performed. After combining the upper organic layer from the two ether extractions, 60 µL of the ether extract and 20 µL of *N-tert*-butyldimethylsilyl-*N*-methyltrifluoroacetamide (MTBSTFA) were mixed in a 100 µL glass insert in a GC auto-sampler vial and incubated for 2 h at room temperature. Samples were analyzed in a randomized order.

Derivatized samples (1 µL) were injected with 15:1 split into an Agilent 7890A gas chromatography system coupled with 5975C mass spectrometer detector (Agilent, CA). Analyses were carried on a HP-5MS capillary column (30 m x 0.25 mm, 0.25 µm film thickness, Agilent J & W Scientific, Folsom, CA) using electronic impact (70 eV) as ionization mode. Helium was used as a carrier gas at a constant flow rate of 1.26 mL/min and the solvent delay time was set to 3.5 min. The column head-pressure was 10 p.s.i. The temperatures of injector, transfer line, and quadrupole were 270°C, 280°C and 150°C, respectively. The GC oven was programmed as follows: 45°C hold for 2.25 min; increase to 200°C at a rate of 20°C/min; increase to 300°C at a rate of 100°C/min; hold for 3 min.

Quantification of SCFAs was performed by isotope dilution GC–MS using selected ion monitoring (SIM). For SIM analysis, the m/z for native and labeled molecular peaks for SCFA quantified were: 117 and 122 (acetate), 131 and 136 (propionate), 145 and 149 (butyrate), 261 and 264 (lactate) and 289 and 293 (succinate), respectively. Various concentrations of standards were spiked into control samples to prepare calibration curves for quantification.

Non-targeted GC-MS - Fecal pellets were weighed and 20 volumes of HPLC grade water were added. Homogenization was performed using a bead beater without beads (mini-beadbeater-8; BioSpec Products; Bartlesville, OK; set on homogenize for 2 min at room temperature). After centrifugation (20,000 x g for 10 min at 4°C), a 200 µL aliquot of the supernatant was transferred to a clean tube and 400 µL of ice-cold methanol was added. The mixture was vortexed vigorously and subsequently centrifuged (20,000 x g for 10 min at 4°C). A 500 µL aliquot of the resulting supernatant was combined with 10 µL of lysine-$^{13}C_6$,$^{15}N_2$ (2 mM) and the mixture dried in a speed vacuum.

Derivatization of all dried supernatants followed a method adapted with modifications from (*49*). Briefly, 80 µL of methoxylamine solution (15 mg/mL in pyridine) was added to methoximate reactive carbonyls and the mixture incubated at 37^{o}C for 16 h. This step was followed by replacement of exchangeable protons with trimethylsilyl groups using *N*-methyl-*N*-(trimethylsilyl) trifluoroacetamide (MSTFA) with a 1% v/v catalytic admixture of trimethylchlorosilane (Thermo-Fisher Scientific, Rockford, IL) (incubated at 70^{o}C for 1 h). Heptane (160 µL) was added and an aliquot of derivatized samples (1 µL) were injected without split into the Agilent 7890A gas chromatography system and coupled 5975C mass spectrometer detector described

above. Analyses were carried on a HP-5MS capillary column (see above) with the following modifications of the protocol described for targeted GC-MS: helium was used at a constant flow rate of 1 mL/min; the solvent delay time was 5.5 min; the column head-pressure was 8.23 p.s.i; the temperatures of the injector, transfer line, and source were 250°C, 290°C and 230°C, respectively; and the GC oven was programmed for a 60 °C hold for 2 min, followed by increases to (i) 140°C at 10°C/min, (ii) 240°C at 4°C/min, and (iii) 300°C at 10°C/min and finally 300°C for 8 min. Metabolites were identified by co-characterization of standards.

Analysis of GC-MS datasets - Data in instrument-specific format (.D) were converted to common data format (.cdf) files using MSD ChemStation (E02.01, Agilent, CA). CDF files were extracted using the Bioinformatics Toolbox in the MATLAB 7.1 (The MathWorks, Inc., Natick, MA), along with custom scripts for alignment of the data in the time domain, and automatic integration and extraction of peak intensities. The resulting dataset included sample information, peak retention time and peak intensities. Data were subsequently mean centered and unit variance was scaled for multivariate analysis.

Quality control of GC-MS data – As noted above, samples were analyzed in a randomized order and metabolite identification was done by co-characterization of standards. Pooled quality control (QC) samples were prepared from 20 μL of each sample and analyzed together with the other samples. The QC samples were also inserted and analyzed every 10 samples. To exclude false positives, raw data for statistically significant metabolites were re-evaluated in MSD ChemStation (E02.01, Agilent, CA).

^{1}H-NMR spectroscopic analyses of urine and plasma - Urinary and plasma samples were analyzed using a Bruker 600 MHz spectrometer (Bruker; Rheinstetten, Germany) and a standard set of protocols (*38*). A total of 25 µL of each sample was well mixed with 30 µL of 0.2 M sodium phosphate buffer [20% deuterium oxide, 0.01% 3-(trimethylsilyl)-[2,2,3,3-$^{2}H_4$]-propionic acid sodium salt (TSP) and 3 mM sodium azide]. 50 µL of the resulting mixture was transferred into a micro-NMR tube with an outer diameter of 1.7 mm. A standard one-dimensional solvent suppression NMR pulse sequence (recycle delay [RD]-90^{o}-t_1-90^{o}-t_m-90^{o}-acquisition) was used to acquire 1-dimensional (1-D) ^{1}H NMR spectral data for both urine and plasma. Additionally, a Carr-Purcell-Meiboom-Gill (CPMG) pulse sequence [RD-90°-(t-180°-t)$_n$-acquisition] was applied to plasma samples to allow visualization of small molecular components without substantial interference of macromolecular signals. A total of 512 scans were collected into 64k data points (1k equals 1024 data points) with a spectral width of 20 ppm.

Multivariate data analysis of 1H-NMR spectral data - ^{1}H NMR spectra obtained from urine and plasma were automatically phased, referenced and baseline-corrected. The resulting NMR spectra (δ 0-10) were imported to MATLAB software and digitized into 20,000 data points with resolution of 0.0005 ppm. The water peak region in urinary spectra (δ 4.7-5.05) and plasma CPMG spectra (δ 4.43-5.15) were removed in order to minimize the effect of the disordered baseline. The urea peak (δ 5.58-6.17) in urinary spectra was also removed, followed by peak alignment (*50*) and normalization to total remaining NMR spectral areas in order to perform further analyses, including principal component analysis (PCA) with a log 2 transformed dataset, orthogonal signal

correction-projection to latent structures-discriminant analysis (O-PLS-DA) using unit variance scaling method, and correlation analysis (SIMCA v13.0 and MATLAB software).

Supplementary Figures

Fig. S1. PCoA of Hellinger distances generated from microbiome KEGG EC profiles of Malawian twin pairs who remained concordant for healthy status and twin pairs who became discordant for kwashiorkor. (**A**) Taken from **Fig. 1A** showing PC1 coordinates of all 308 sequenced co-twin fecal microbiomes plotted against age. Each sphere represents a microbiome colored by the age of the human donor. (**B**) Same as panel A but colored by the health status of a twin pair (green, concordant for healthy; red, discordant for kwashiorkor). (**C**) PC1 coordinates of fecal microbiomes from twin pairs discordant for kwashiorkor (n=215 microbiomes) plotted against age, colored by the health status of each co-twin (those who developed kwashiorkor over the course of the study are colored in red before and after onset of the disease; healthy co-twin samples are colored black).

Fig. S2. Hellinger distances within and between the fecal microbiomes of Malawian twin pairs who remained healthy, and twin pairs who became discordant for kwashiorkor. Hellinger distances were derived from the KEGG EC profiles of healthy twin pairs (black bars) and twin pairs discordant for kwashiorkor (red bars). Distances between all microbiomes that originate from a given child, and distances between microbiomes sampled from a given twin pair, are plotted next to the average distance between microbiomes from unrelated children. $p<0.0001$, unpaired Student's t-test with Bonferroni correction.

Fig. S3. Relative abundance of Actinobacteria in the fecal microbiomes of healthy twin pairs and twin pairs discordant for kwashiorkor. Percent relative abundance of Actinobacteria in the fecal microbiome decreases significantly with 2 weeks of RUTF

treatment in co-twins with kwashiorkor but not in their healthy co-twins; *p<0.05 Friedman test with Dunn's post hoc test. Data were generated by blasting shotgun reads against a database of 462 sequenced human gut microbial genomes.

Fig. S4. Anthropometric measurements, health status, and functional composition of the fecal microbiomes of twin pairs from families 196, 57, and 56. Anthropometric Z scores, episodes of diarrhea, fever, cough and vomiting, relative abundance of major bacteria taxa based on the BLAST analysis to 462 bacterial genomes for twin pair 196 (**A-C**), twin pair 57 (**D-F**), and twin pair 56 (**G-I**). The DZ male co-twins from family 196 were enrolled from the village of Chamba at 2.7-months of age when both were healthy. Their last visit took place when they were 34.7-months old. There were no symptoms of cough, fever, diarrhea or vomiting at the time when the co-twin with kwashiorkor first presented with his disease. The MZ female co-twins from family 57 were enrolled from the village Mbiza at 20.6-months of age when both were healthy. Their last visit took place when they were 36.2 months old. At the time of presentation of kwashiorkor, the affected female presented with two days of fever preceding the clinic visit. The MZ female co-twins from family 56 were enrolled from the village Mbiza at 17.2 months of age when both were healthy. Their last visit took place when they were 36.3 months old. The number of episodes of fever, cough, diarrhea and vomiting were similar between the co-twins and was not higher in the child who developed kwashiorkor, either before or at the time of presentation with the disease.

Fig. S5. Sampling scheme for gnotobiotic mouse recipients of fecal microbiota transplants from discordant twin pair 196. A star designates the time point at which a sample was used for the indicated analysis.

Fig. S6. Efficient transmission of microbiome functions from human donors to recipient gnotobiotic mice. (**A**) Correlation between the percent relative KEGG EC abundance in the input fecal microbiomes of twins belonging to discordant pair 196 and those in the output fecal microbiomes of mice three weeks after gavage while animals were consuming a Malawian diet (M1 phase; mean values ± SEM shown). (**B**) R-squared values for input fecal microbiomes versus microbiomes of individual recipient mice in panel A. (**C**,**D**) Comparable data as in panels A and B but in this case from co-twins belonging to discordant pair 57.

Fig. S7. PCR-Luminex assays of enteropathogens in human fecal microbota donor samples from families 196 and 57, and in mouse experiments involving fecal microbiota transplants from discordant twins in family 196. (A) Fecal samples collected from family 196 and family 57 donors, at the time that the co-twin was diagnosed with kwashiorkor. **(B)** Assays of atypical enteropathogenic *E. coli* (eae) and enterotoxigenic E. coli (STh and LT) in input human donor fecal samples and fecal samples collected from gnotobiotic mice at the indicated time points on the indicated diets. **(C)** Assay of *Cryptosporidium* in the same samples used in panel B. *Cryptosporidium* DNA appeared in one gnotobiotic mouse recipient of the kwashiorkor co-twin's microbiota 19 days after gavage and became undetectable shortly after treatment with RUTF was initiated. The degree of weight loss in this animal on the Malawian diet was not greater than other members of this treatment group. Corrected median fluorescence intensity (cMFI), a measure of amplicon quantity, is shown on the y-axes.

Fig. S8. Weighted UniFrac-based PCoA plots of changes in the phylogenetic configurations of the fecal microbiota of gnotobiotic mice containing transplanted gut microbial communities from discordant pairs 196 (A, B) and 57 (C, D). Spheres represent a single mouse fecal community, and are colored by donor microbiota and diet: healthy microbiota recipients consuming a Malawian diet (red) or RUTF (blue); kwashiorkor microbiota recipients consuming a Malawian diet (orange) or RUTF (green).

Fig. S9. Non-targeted GC-MS analysis of metabolites in fecal samples collected from mice with transplanted microbiota from discordant pair 196. (**A,B**) PCoA plots, based on Hellinger distance measurements, showing the effects of diet on the metabolic profile. (**C**) Heatmap showing Z scores of metabolites with statistically significant differences in their levels as a function of diet ($p<0.05$, unpaired t-test). Samples are grouped based on unsupervised hierarchical clustering of metabolite profiles. The results reveal that within a 'donor-diet' cluster, there is distinction between fecal samples obtained during the first versus second exposures to the Malawian diet (M1 and M2) as well as early versus late during the course of RUTF treatment [day 2 (D02) compared to day 10 (D10)]. Color code: blue, fecal microbiota from gnotobiotic recipients of the kwashiorkor co-twin's microbiota; red, recipients of the healthy co-twin's microbiota.

Fig. S10. Fecal metabolites differentially affected by diet changes in mice harboring transplanted healthy versus kwashiorkor co-twin fecal microbiota. (**A**) Essential amino acids. (**B**) Non-essential amino acids. (**C**) Urea cycle components. The statistical significance of differences observed in pairwise comparisons between the healthy and

kwashiorkor treatment group on a given day of a given diet was evaluated using a two-tailed Student's t-test. Mean values ± SEM are plotted; $p<0.05$.

Fig. S11. Changes in fecal short chain fatty acid and mono- and disaccharide levels as a function of donor microbiota and diet. (**A**) SCFA. (**B**) Mono- and disaccharides. The statistical significance in pairwise comparisons between the healthy and kwashiorkor treatment group on a given day of a given diet was evaluated using a two-tailed Student's t-test. Mean values ± SEM are plotted; $p<0.05$.

Fig. S12. **Procrustes analysis showing correlation between the bacterial phylogenetic configurations and metabolic profiles of fecal samples from mice containing transplanted microbiota from discordant co-twins in family 196.** Every sphere represents a single mouse fecal community. For a given type of data, fecal microbiota were compared using Hellinger distance measurements. The grey end of each line is connected to metabolic data, while the red end is connected to the V4-16S rRNA data. The M^2 value of 0.380 is the fit of the Procrustes transformation over the first three dimensions and is statistically significant ($p<0.0001$, based on 1000 Monte Carlo simulations). (**A**) Spheres colored based on donor: blue, recipients of the kwashiorkor co-twin's microbiota; red, recipients of the healthy co-twin's microbiota. (**B**) Spheres are colored based on diet: red, first Malawian diet period; orange, RUTF; blue, second Malawian diet period.

Fig. S13. Non-targeted GC-MS analysis of metabolites in fecal samples collected from mice with transplanted microbiota from discordant pair 57. Heatmap of Z scores showing metabolites with significant differences in their levels as a function of diet ($p<0.05$, unpaired t-test). Samples are grouped based on unsupervised hierarchical

clustering. The results reveal that within a 'donor-diet' cluster, there is distinction between fecal samples obtained during the first and second exposures to the Malawian diet (M1 and M2).

Supplementary Tables

Table S1. Characteristics of twins with acute malnutrition.

Table S2. Fecal metagenomic datasets obtained from healthy twin pairs, from twin pairs discordant for kwashiorkor and from mice that were the recipients of human fecal microbiota transplants.

Table S3. List of 462 sequenced human gut-derived microbial genomes used for analysis of shotgun sequencing datasets.

Table S4. Results of the linear mixed-effects regression of PC1, derived from KEGG EC profiles of 308 human microbiomes, with age.

Table S5. ECs with significant differences in their representation in the fecal microbiomes of co-twins in each twin pair discordant for kwashiorkor, before diagnosis of kwashiorkor, at time of diagnosis of kwashiorkor, 2 weeks after initiation of RUTF, and 1 month after cessation of RUTF.

Table S6. Nutrient analysis of the Malawian and RUTF diets used in this study along with nutritional requirements for mice and 1-3 year old humans.

Table S7. Proportional representation of species-level taxa in human donor microbiota and in fecal samples obtained from gnotobiotic mouse recipients over time during each diet period.

Table S8. Species-level taxa whose proportional representation was significantly different between gnotobiotic mouse recipients of a healthy versus kwashiorkor co-twin microbiota transplant, as a function of diet.

Table S9. Bacterial taxa whose proportional representation changed significantly as a function of diet in gnotobiotic mouse recipients of fecal microbiota transplants from both families 196 and 57 compared to changes observed in the other 11 discordant twin pairs.

Table S10. Changes of metabolites observed in urinary samples obtained from mice with transplanted healthy or kwashiorkor co-twin microbiota from families 196 and 57 at each diet phase (M1, RUTF, M2).

Smith_Yatsunenko Fig. 1

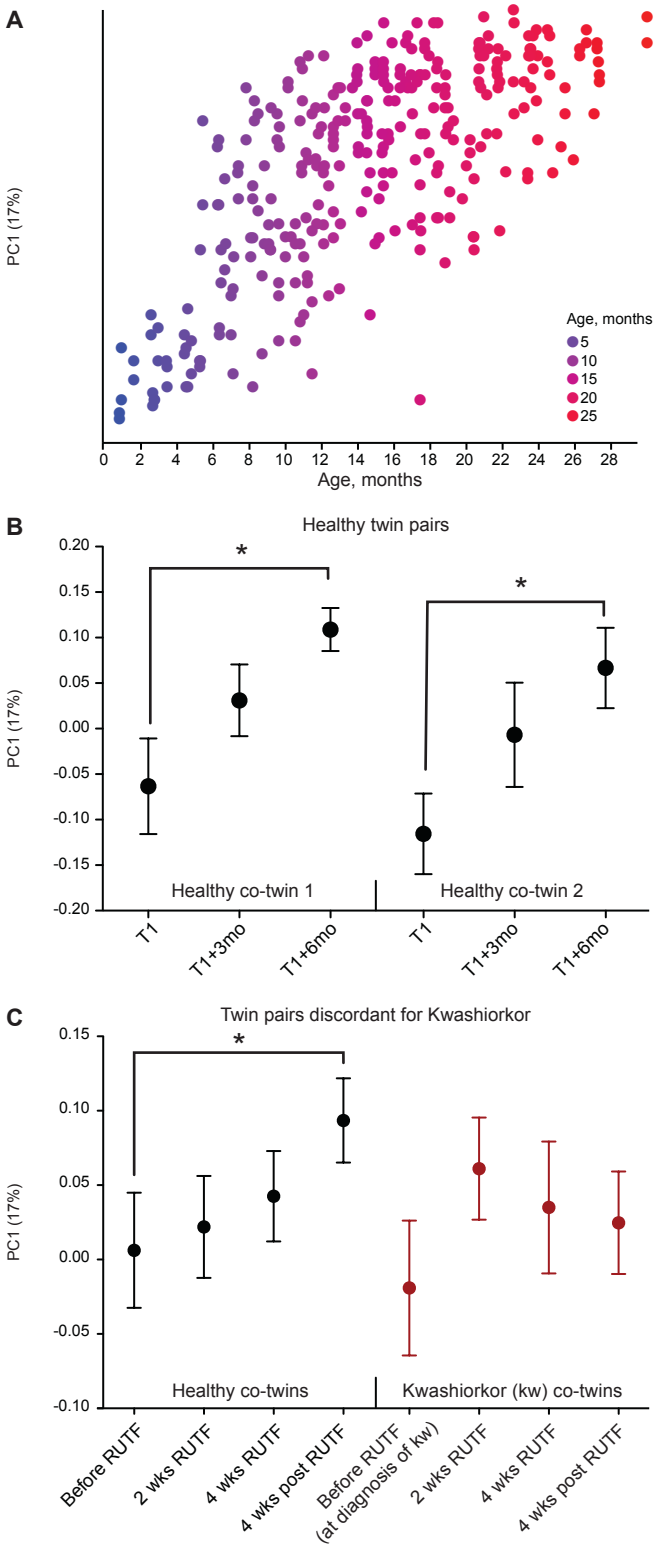

Smith_Yatsunenko Fig. 2

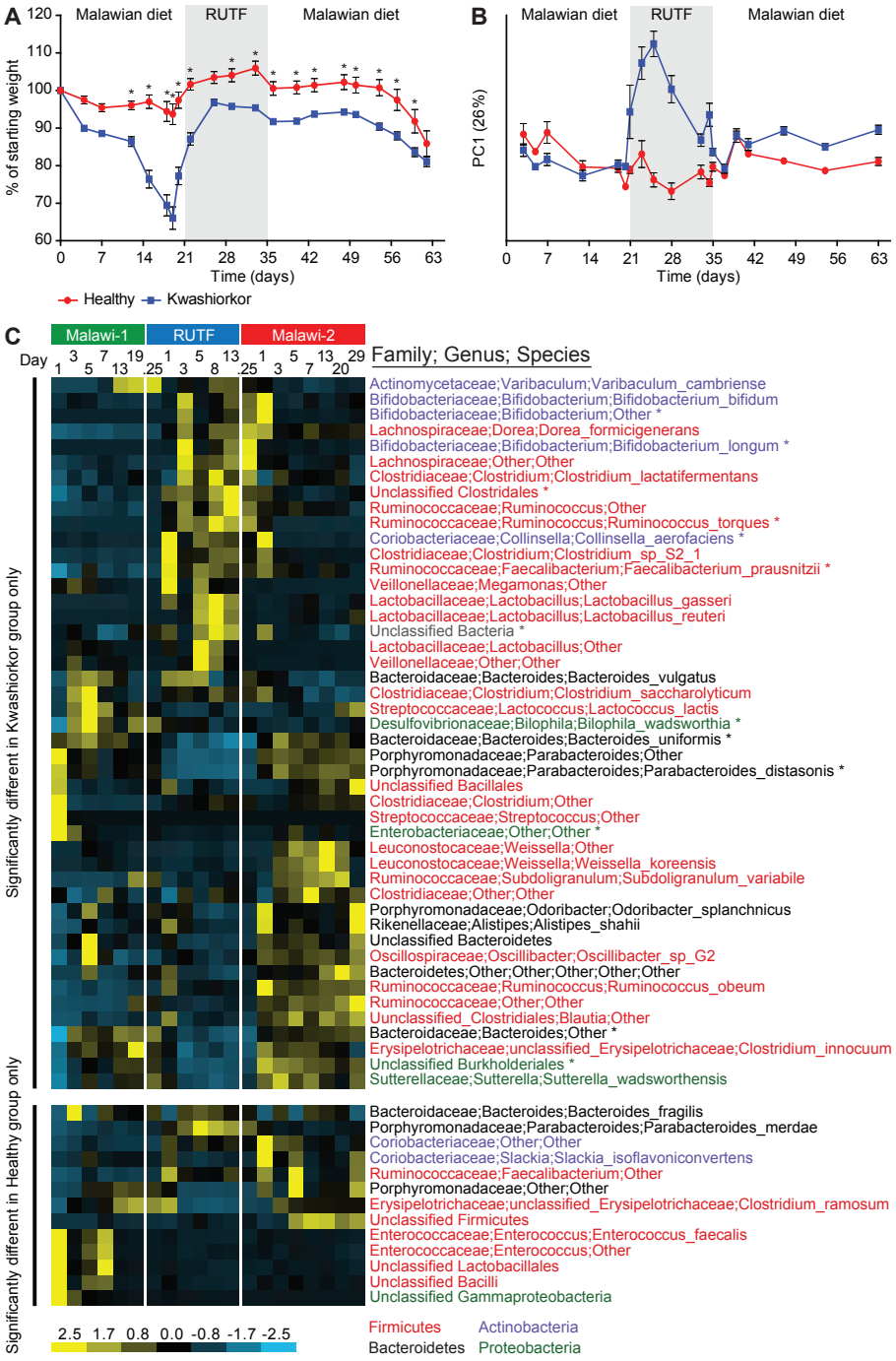

Smith_Yatsunenko Fig. 3

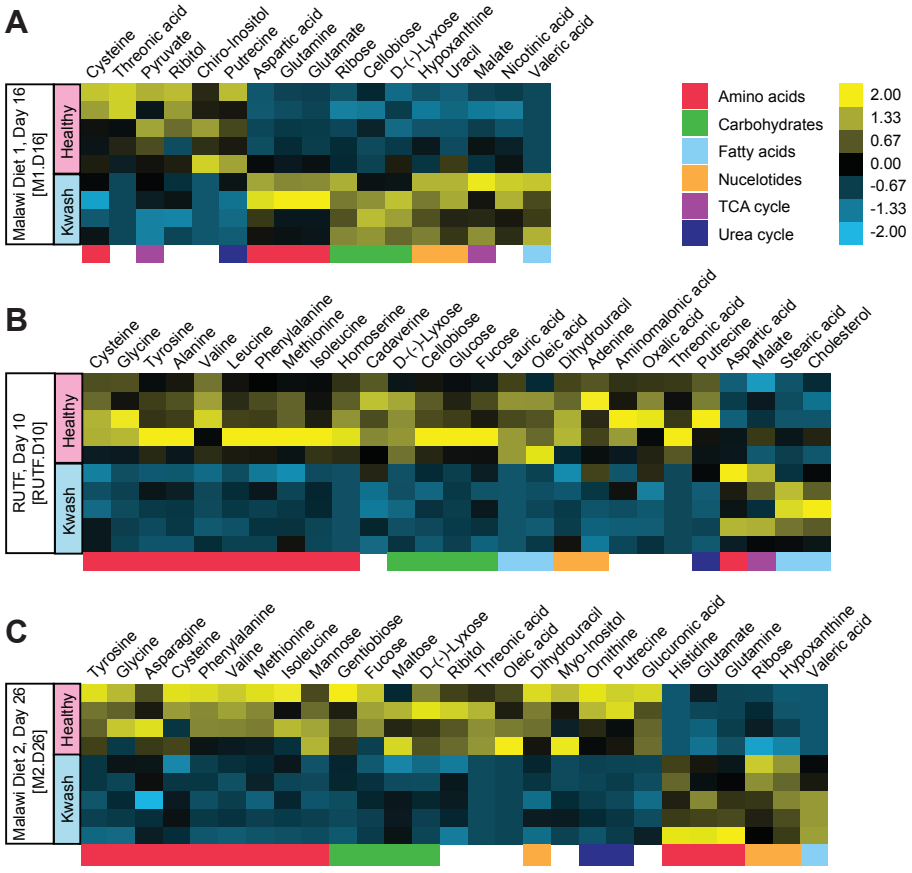

Smith_Yatsunenko Fig. 4

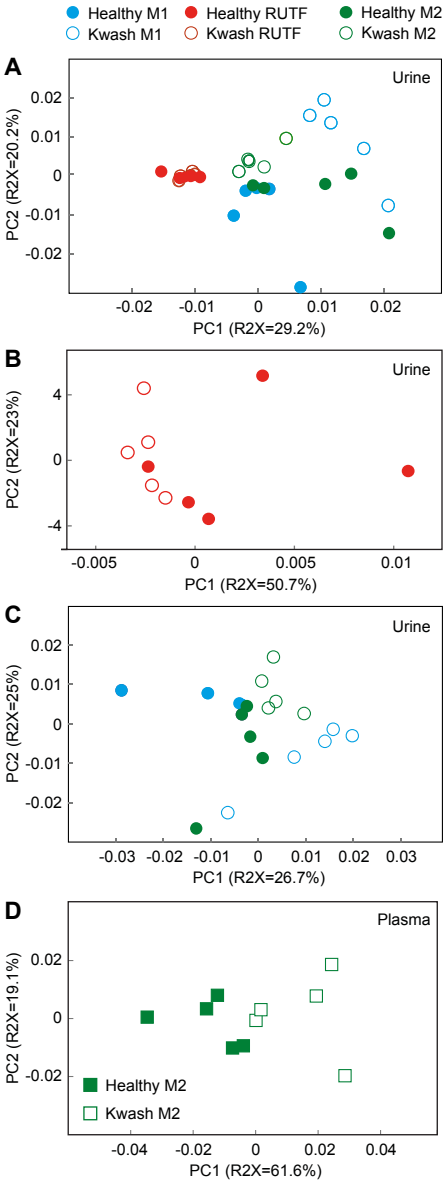

Smith_Yatsunenko Fig. S1

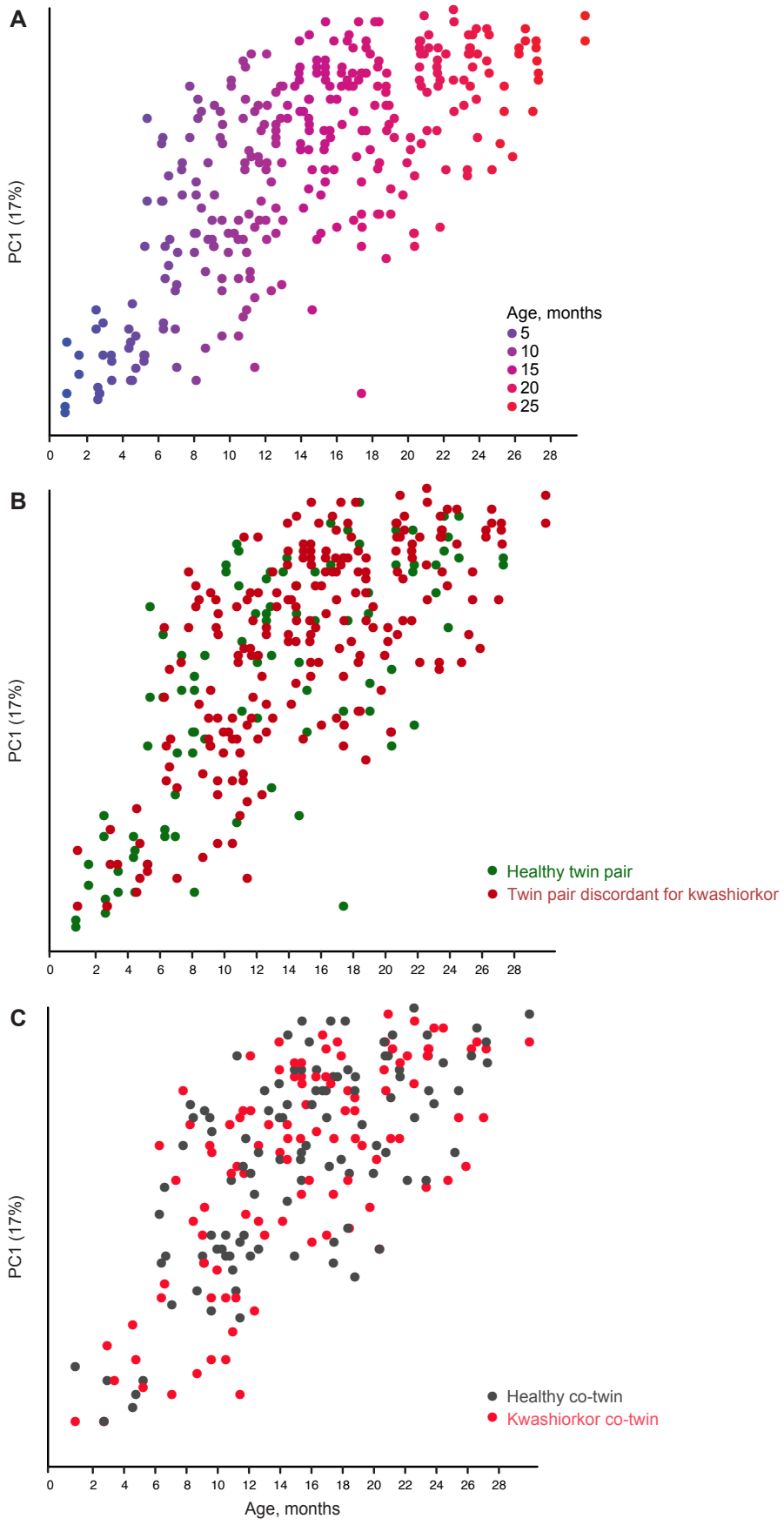

Smith_Yatsunenko Fig. S2

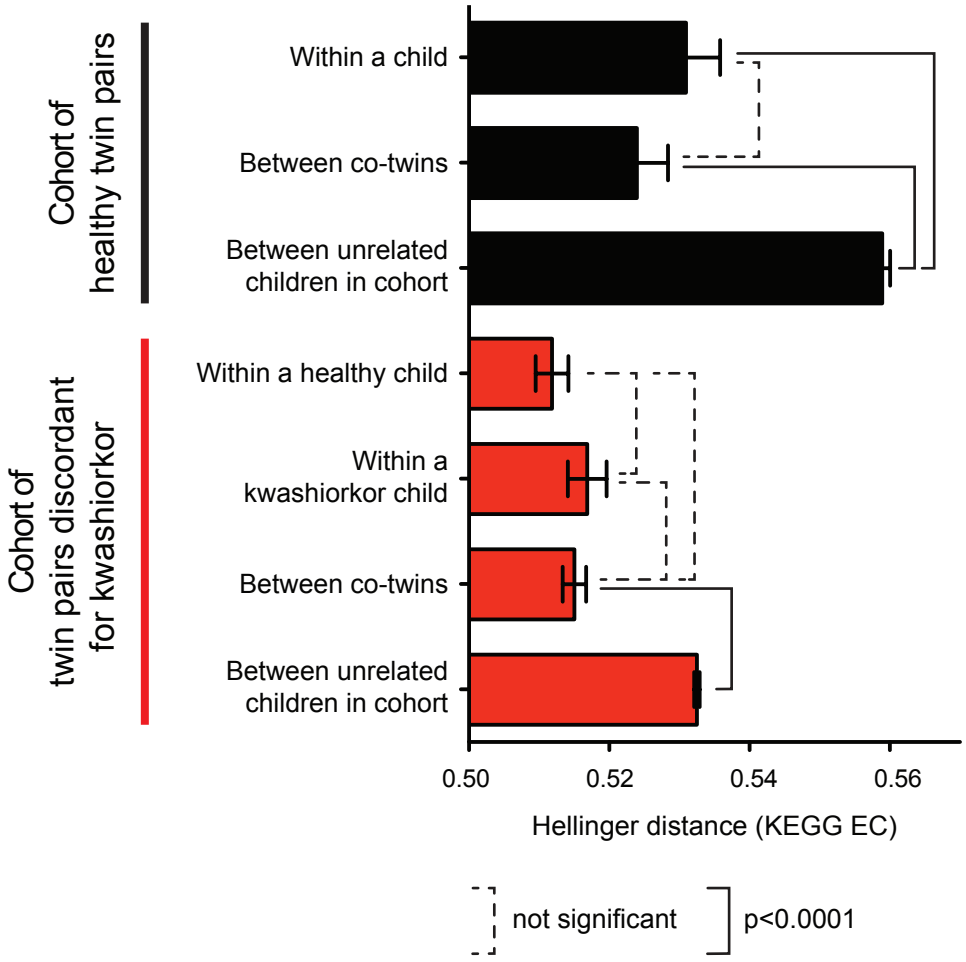

Smith_Yatsunenko Fig. S3

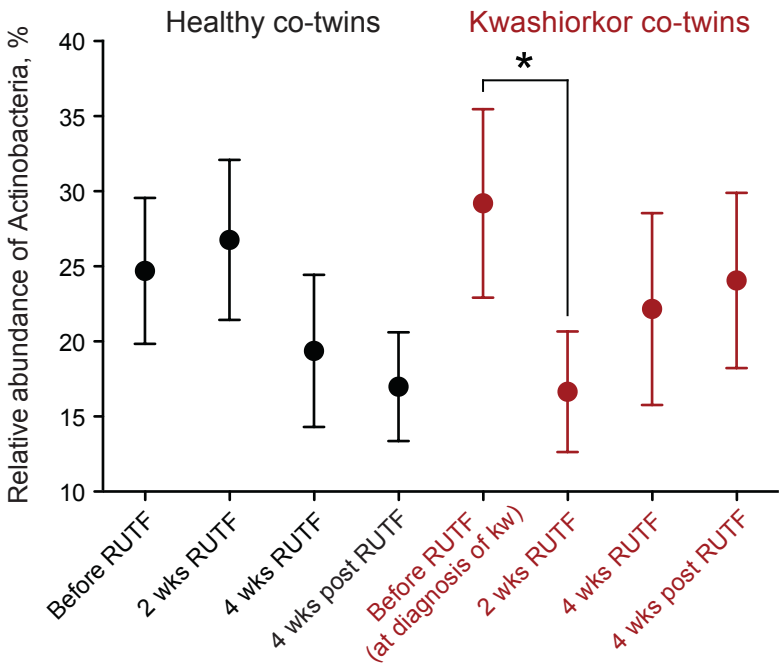

Smith_Yatsunenko Fig. S4

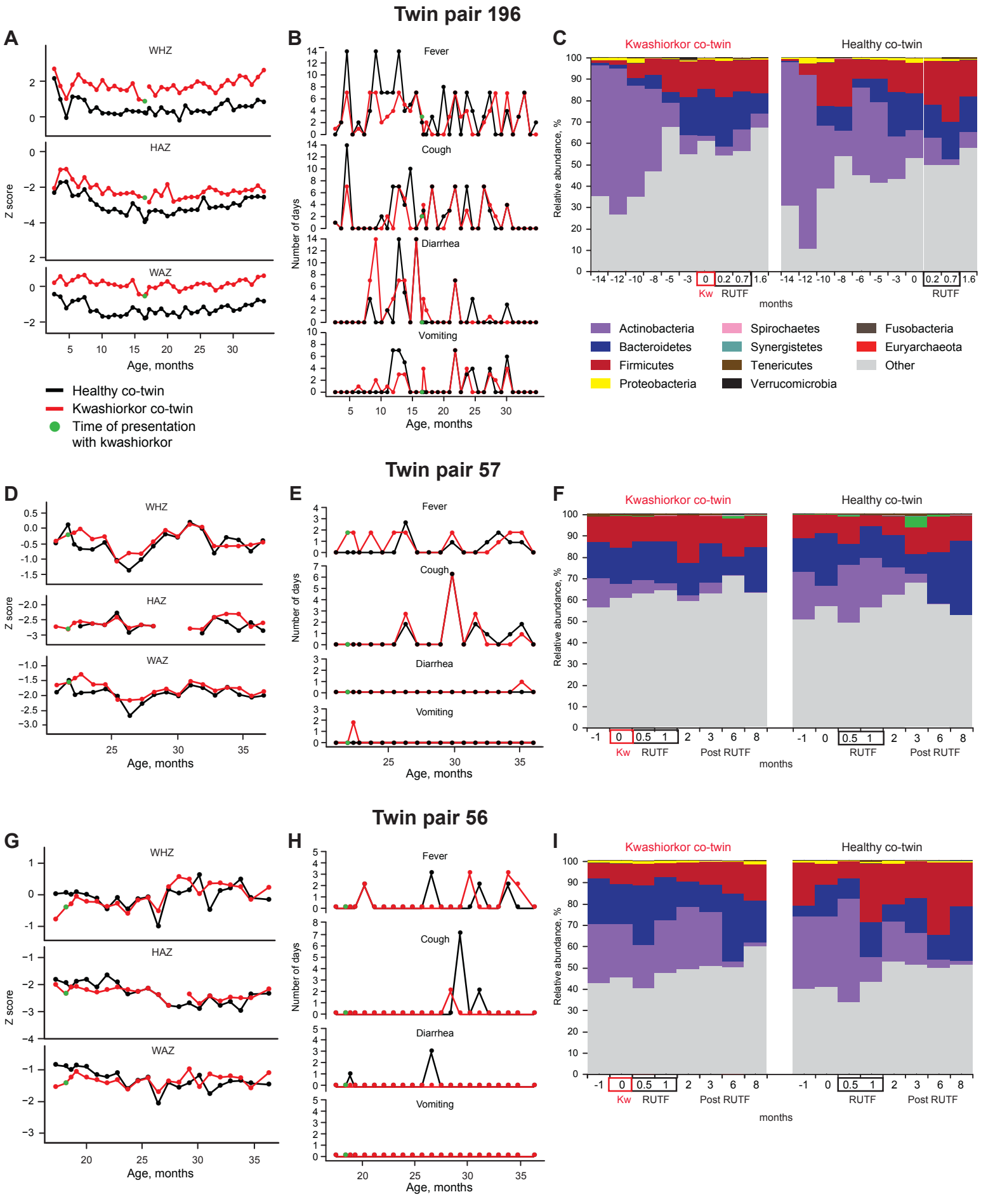

Smith_Yatsunenko Fig.S5

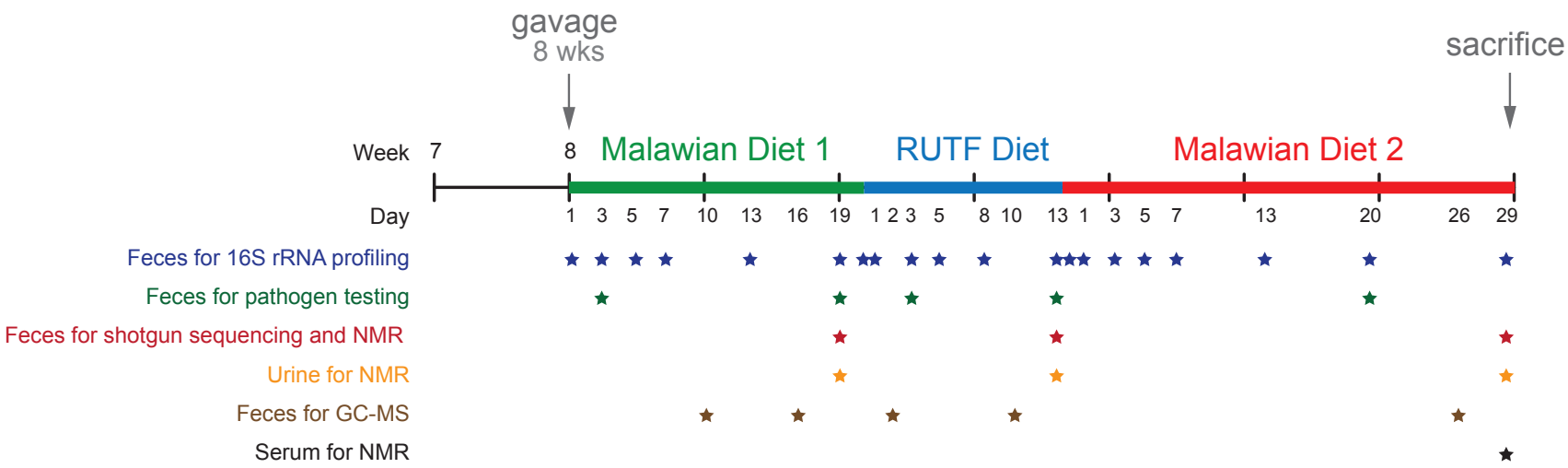

Smith_Yatsunenko Fig. S6

A

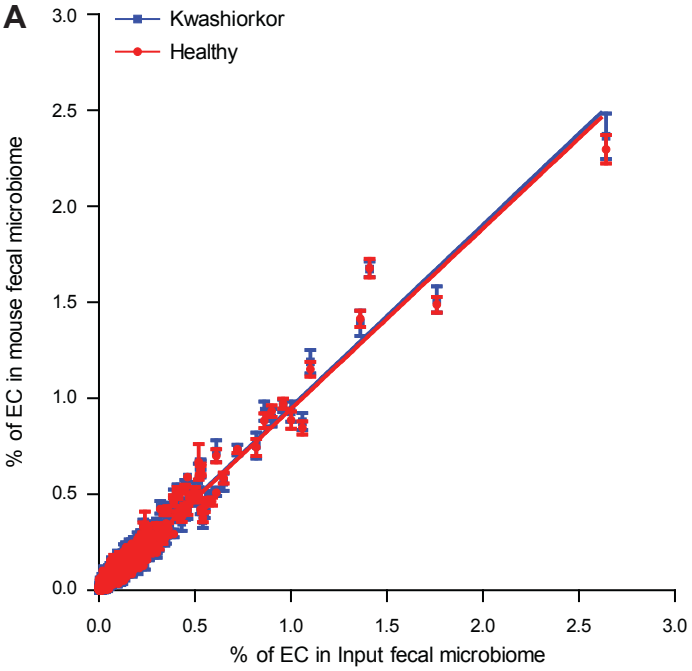

B

Correlation of % EC abundance in input donor sample microbiome versus microbiome of recipient mice consuming a Malawian diet 19 days after gavage

Input Sample	Sample ID	R square	Sy.x
Family 196 - kwashiorkor co-twin	k196A.M1.D19.k3.F	0.9195	0.042
	k196A.M1.D19.k4.F	0.92	0.04088
	k196A.M1.D19.k6.F	0.9351	0.03793
	k196A.M1.D19.k7.F	0.923	0.04123
	k196A.M1.D19.k8.F	0.9358	0.038
Family 196 - healthy co-twin	h196B.M1.D19.h10.F	0.9195	0.042
	h196B.M1.D19.h2.F	0.92	0.04088
	h196B.M1.D19.h3.F	0.9351	0.03793
	h196B.M1.D19.h4.F	0.923	0.04123
	h196B.M1.D19.h5.F	0.9358	0.038
	h196B.M1.D19.h6.F	0.933	0.03751
	h196B.M1.D19.h7.F	0.9236	0.03882
	h196B.M1.D19.h8.F	0.8933	0.04835
	h196B.M1.D19.h9.F	0.9229	0.04068

C

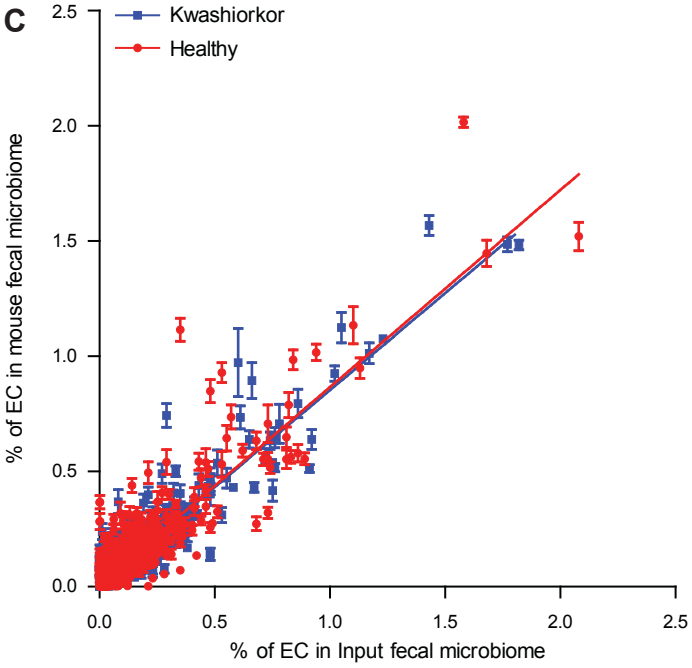

D

Correlation of % EC abundance in input donor sample microbiome versus microbiome of recipient mice consuming a Malawian diet 19 days after gavage

Input Sample	Sample ID	R square	Sy.x
Family 57 - kwashiorkor co-twin	k57A.M1.D19.k1.F	0.859	0.05032
	k57A.M1.D19.k2.F	0.849	0.05225
	k57A.M1.D19.k3.F	0.8443	0.05271
	k57A.M1.D19.k4.F	0.7992	0.06039
	k57A.M1.D19.k5.F	0.8472	0.05276
Family 57 - healthy co-twin	h57B.M1.D19.h1.F	0.801	0.06463
	h57B.M1.D19.h2.F	0.7922	0.0631
	h57B.M1.D19.h3.F	0.786	0.06609
	h57B.M1.D19.h4.F	0.7838	0.06556
	h57B.M1.D19.h5.F	0.8062	0.06141

Smith_Yatsunenko Fig. S7

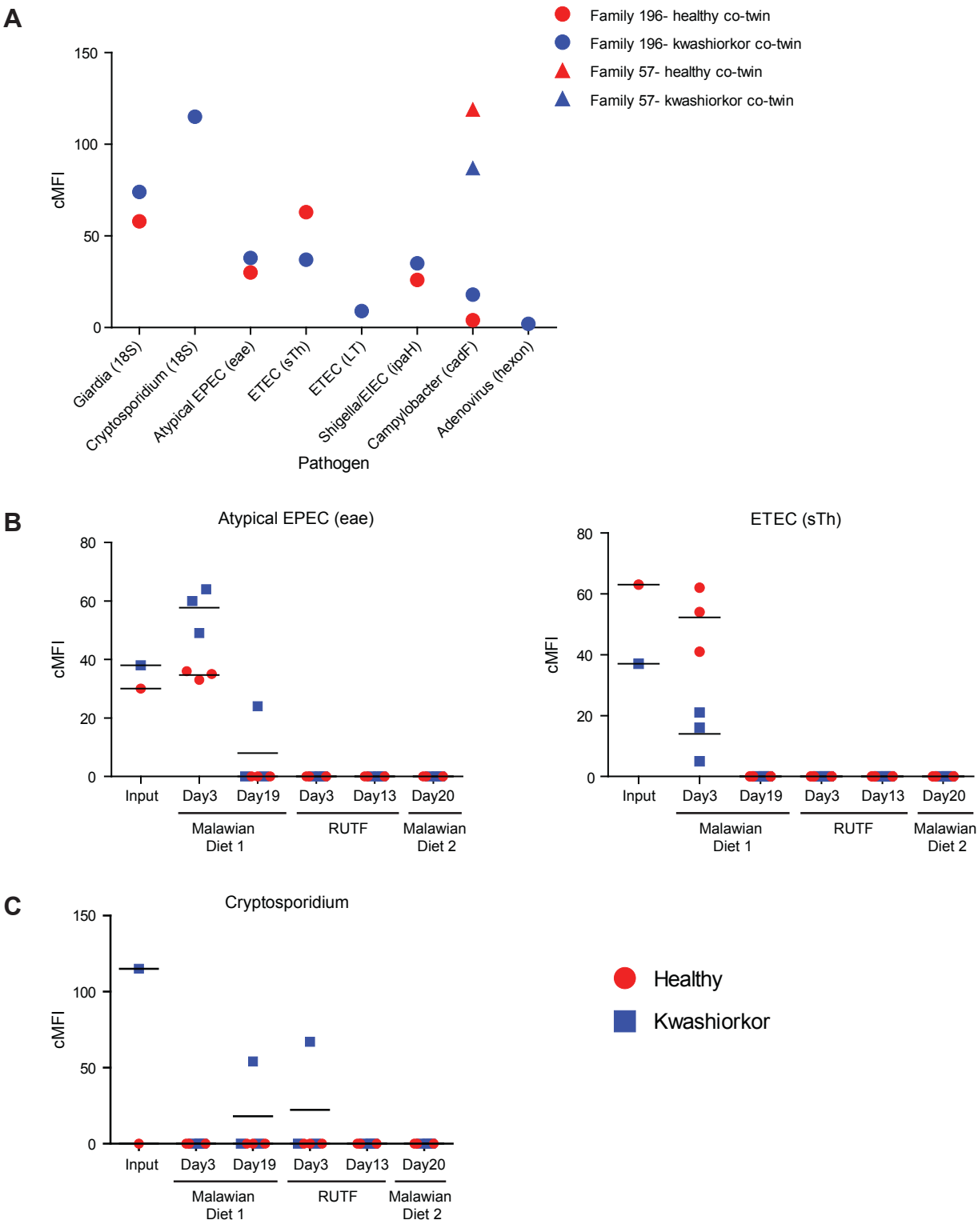

Smith_Yatsunenko Fig. S8

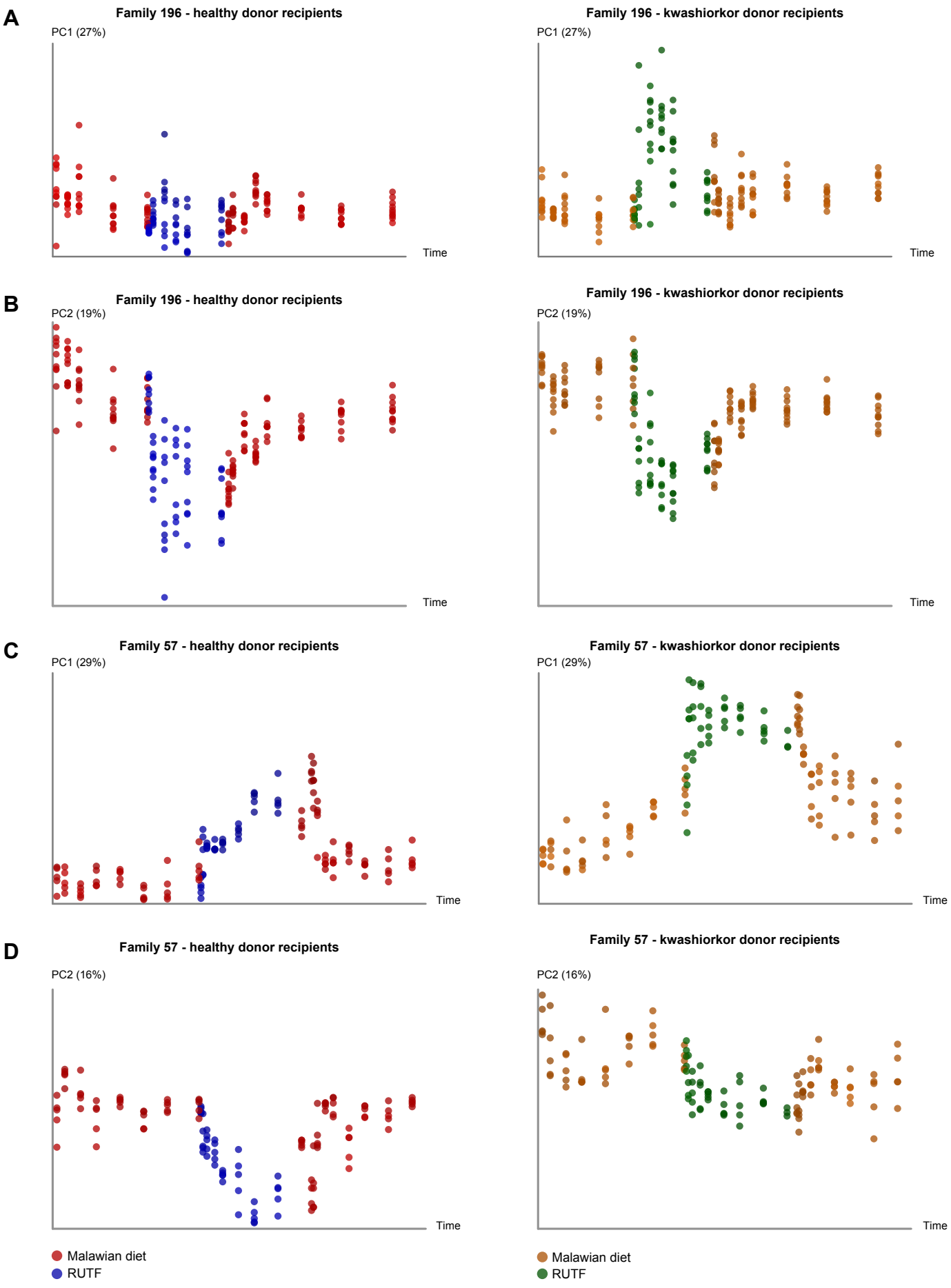

Smith_Yatsunenko Fig. S9

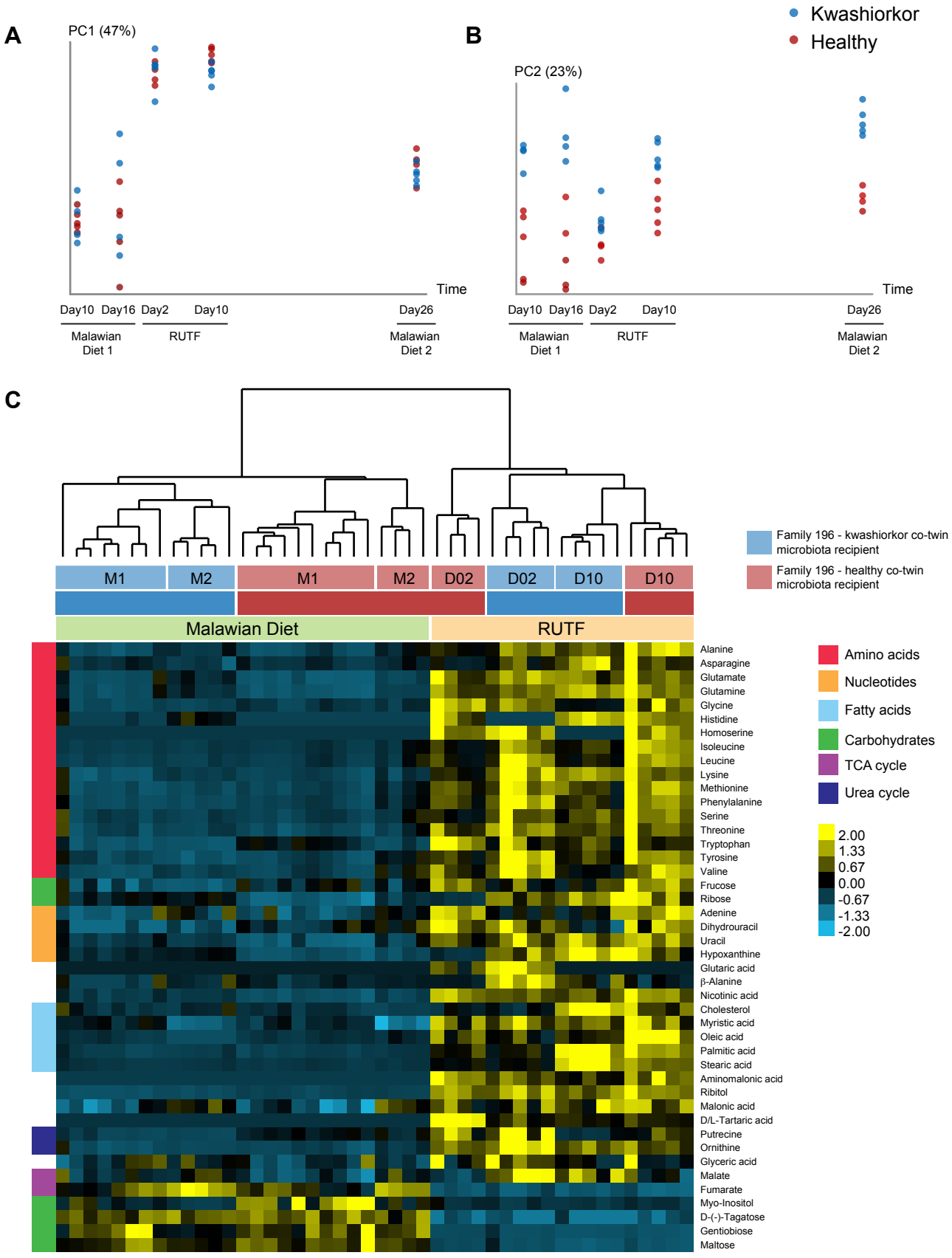

Smith_Yatsunenko Fig. S10

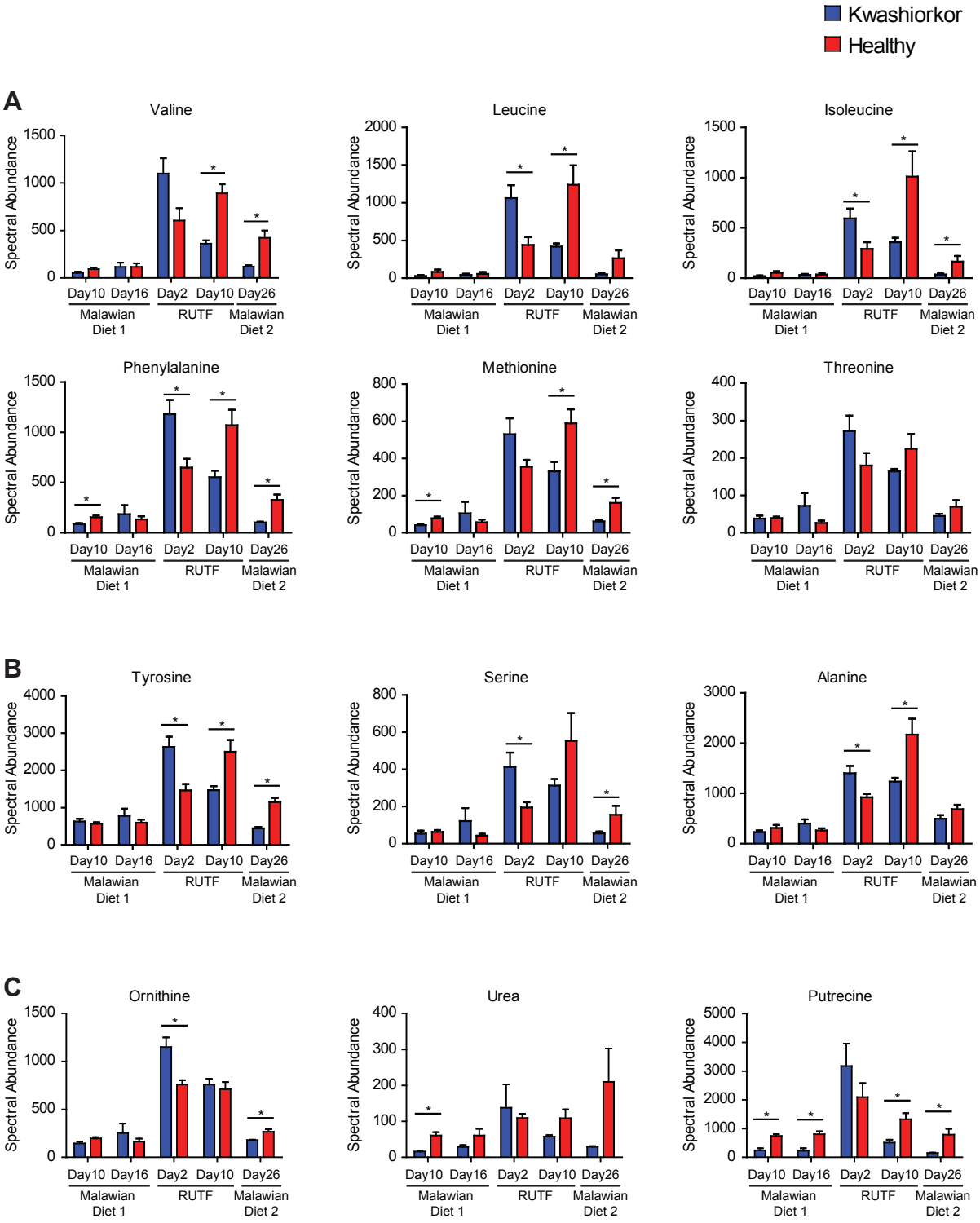

Smith_Yatsunenko Fig. S11

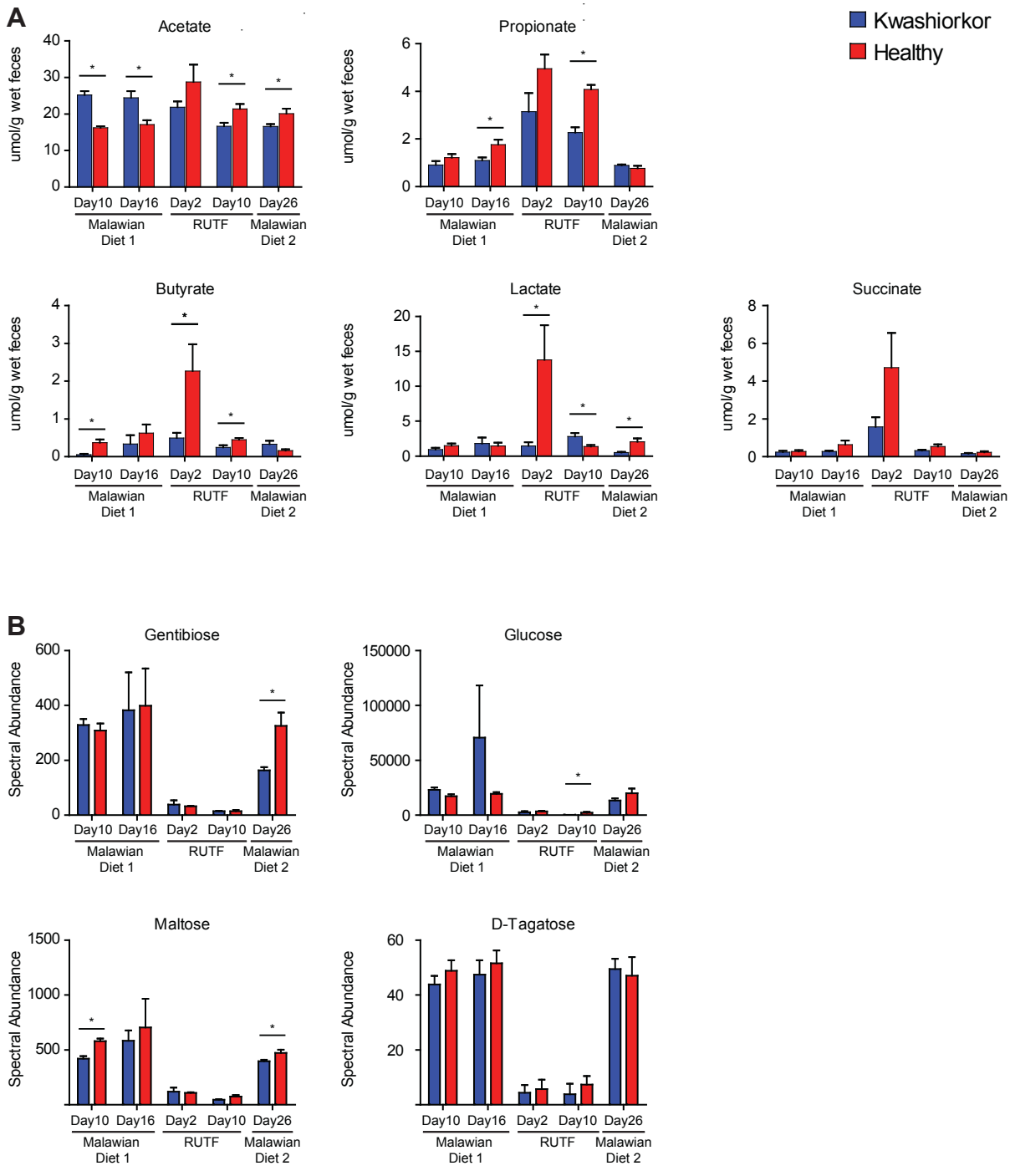

Smith_Yatsunenko Fig. S12

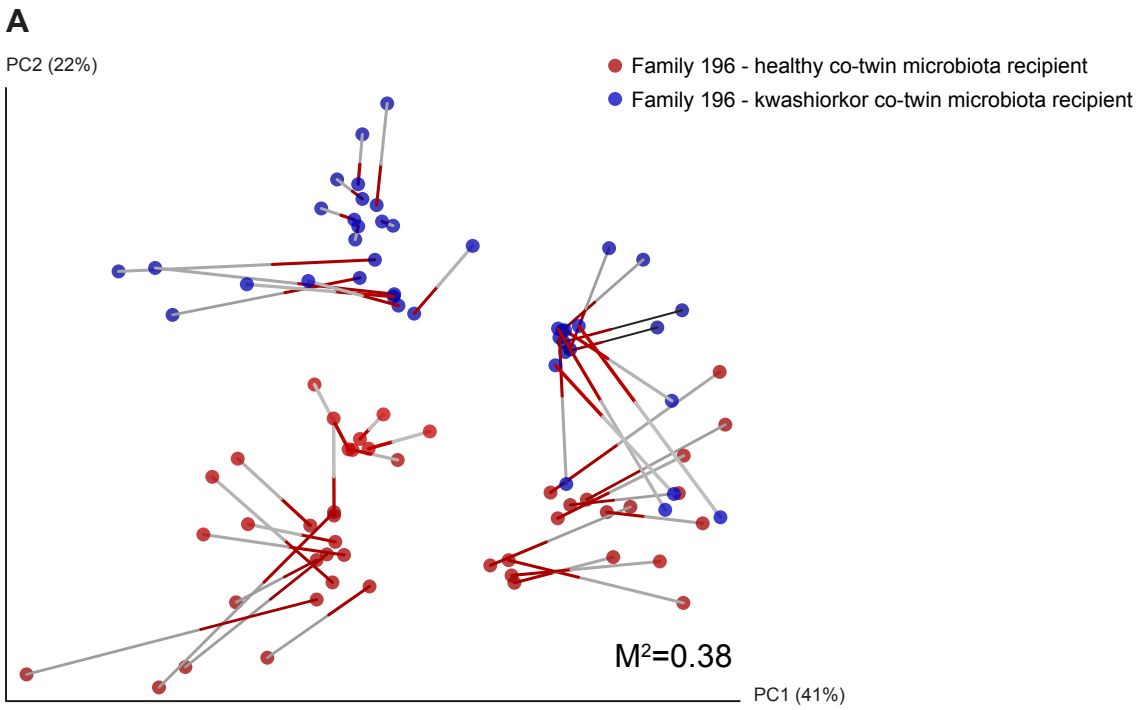

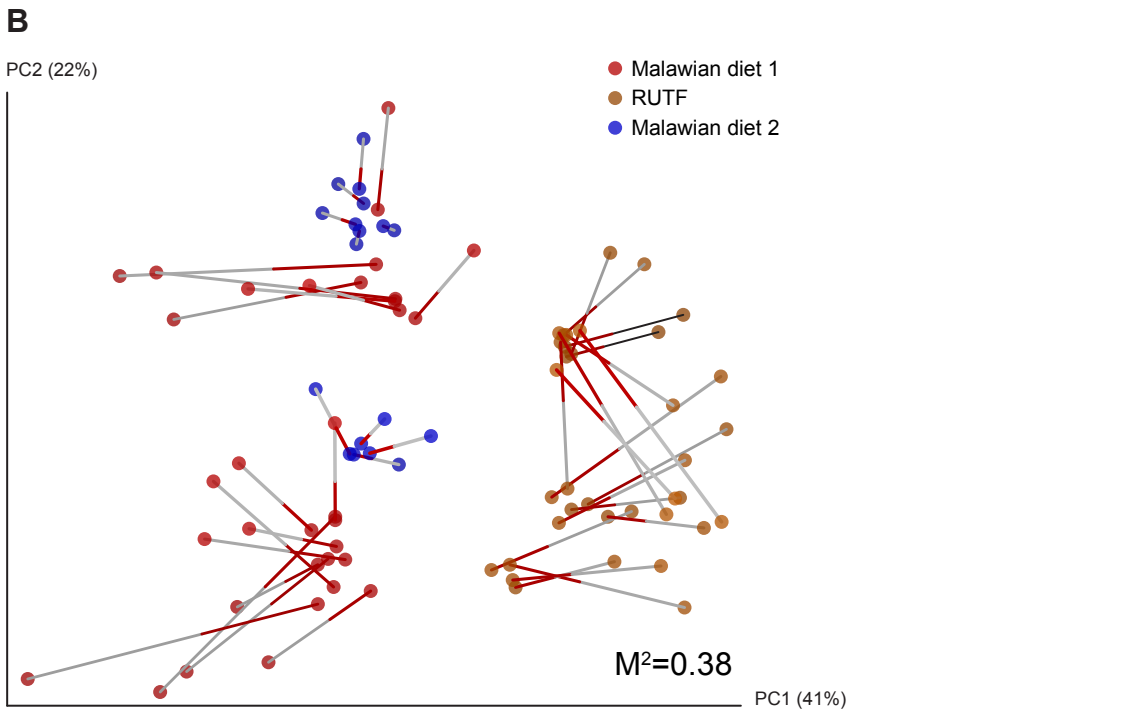

Smith_Yatsunenko Fig. S13